

Description of the uEMEP_v5 downscaling approach for the EMEP MSC-W chemistry transport model

Bruce Rolstad Denby¹, Michael Gauss¹, Peter Wind^{1,2}, Qing Mu¹, Eivind Grøtting Wærsted¹, Hilde Fagerli¹, Alvaro Valdebenito¹, Heiko Klein¹

5 ¹ The Norwegian Meteorological Institute, Henrik Mohns Plass 1, 0313, Oslo, Norway

² Department of Chemistry, UiT - The Arctic University of Norway, N-9037 Tromsø, Norway

Correspondence to: Bruce Rolstad Denby (brucerd@met.no)

Abstract. A description of the new air quality downscaling model uEMEP and its combination with the EMEP MSC-W chemistry transport model is presented. uEMEP is based on well known Gaussian modelling principles. The uniqueness of the system is in its combination with the EMEP MSC-W model and the ‘local fraction’ calculation contained within it. This allows the uEMEP model to be imbedded in the EMEP MSC-W model and downscaling can be carried out anywhere within the EMEP model domain, without any double counting of emissions, if appropriate proxy data is available that describe the spatial distribution of the emissions. This makes the model suitable for high resolution calculations, down to 50 m, over entire countries. An example application, the Norwegian air quality forecasting and assessment system, is described where the entire country is modelled at a resolution of between 250 and 50 m. The model is validated against all available monitoring data, including traffic sites, in Norway. The results of the validation show good results for NO₂, which has the best known emissions, and moderately good for PM₁₀ and PM_{2.5}. In Norway the largest contributor to PM, even in cities, is long range transport followed by road dust and domestic heating emissions. These contributors to PM are more difficult to quantify than NO_x exhaust emission from traffic, which is the major contributor to NO₂ concentrations. In addition to the validation results a number of verification and sensitivity results are summarised. One verification showed that single annual mean calculations with a rotationally symmetric dispersion kernel give very similar results to the average of an entire year of hourly calculations, reducing the run time for annual means by four orders of magnitude. The uEMEP model, in combination with EMEP MSC-W model, provides a new tool for assessing local scale concentrations and exposure over large regions in a consistent and homogenous way and is suitable for large scale policy applications.

25

1. Introduction

The EMEP MSC-W model is a chemistry transport model, which has been developed by the Meteorological Synthesizing Centre - West (MSC-W) of EMEP, the European Monitoring and Evaluation Programme under the UN Convention on Long-range Transboundary Air pollution (LRTAP). It is documented in Simpson et al. (2012) and has been used for many years mainly for regional but also for global applications. The aim of uEMEP (urban EMEP) is to further extend the application of the EMEP MSC-W chemical transport model down to near street level modelling. The downscaling methodology builds on classical Gaussian plume modelling and is integrated with the EMEP MSC-W models physical parameterisations and emission data in such a way as to provide a consistent model description from regional to local scales. Unlike other urban scale models uEMEP is intended not just to achieve local scale modelling for one individual city or area but to provide local scale modelling over entire countries or continents, providing high resolution modelling over large areas and allowing air quality assessment and exposure calculations at high resolution everywhere.

Air quality modelling is often separated into global, regional, urban and local scales. In this context local refers to the ability of the model not just to represent urban background concentrations but also to represent street level concentrations. There are a number of models that span the global or regional scale where grid resolutions down to 4-10 km have been achieved, e.g. EMEP MSC-W (Simpson et al., 2012; Werner et al., 2018), CHIMERE (Menuet et al., 2013), SILAM (Sofiev et al., 2015), LOTOS-EUROS (Kranenburg et al., 2013), MATCH (Andersson et al., 2007) and CMAQ (Appel et al., 2017). There are a number of Gaussian modelling systems that cover the urban and local scales over limited areas, usually individual cities, e.g. ADMS (Stocker et al., 2012) and AERMOD (Cimorelli et al., 2004). In addition there are some limited area models that combine Eulerian and Gaussian plume type models in a single system, e.g. Karamchandani et al. (2009), Kim et al. (2018) and Karl et al. (2019). If the full model cascade is to be achieved, such as the THOR forecast system in Denmark (Brandt et al., 2001), then this requires linking different model systems together to achieve high resolution calculations in a limited area. An alternative approach to achieving high resolution concentration fields over large regions without the use of CTMs (Chemical transport models) are land use regression methods (e.g. Vizcaino and Lavallo, 2018), however their lack of underlying physics do not make them useful for planning or policy applications.

Earlier work on the downscaling of CTM models over large regions include the population covariance correction factor from Denby et al. (2011) and the dispersion kernel methods from Theobald et al. (2016) and Maiheu et al. (2017). There are similarities between uEMEP and these last two studies as both use Gaussian models for the downscaling. The major difference between uEMEP and these two Gaussian kernel methods is that uEMEP can be applied on hourly data, as well as annual data, and that uEMEP is integrated with the 'local fraction' scheme in EMEP MSC-W (Wind et al., 2020) that avoids double counting of emissions in a consistent manner.

60

In this paper we provide an overall description of the uEMEP methodology and how it is combined with the ‘local fraction’ scheme in EMEP MSC-W (Sect. 2). The uEMEP model physical parameterisations are then given in Sect. 3. In Sect. 4 an application example of the methodology, the Norwegian air quality forecasting service, is described. Validation of the modelling system against all Norwegian monitoring data is presented in Sect. 5 together with a summary of verification and sensitivity studies. Various aspects of the modelling are discussed in Sect. 6 and conclusions made in Sect. 7. Supplementary material providing more detailed information on the parameterisations, validation and verification is also provided.

2. Methodology

In this section we describe the concepts and methodologies for the application of the coupled modelling system uEMEP and EMEP MSC-W.

2.1 Overall concept and methodology

uEMEP provides a consistent methodology for redistributing/downscaling gridded CTM emissions and concentrations, in this case from the EMEP MSC-W model, to higher resolution sub-grids within the CTM grids. Proxy data, that represent the spatial distribution of the emissions, are used to redistribute emissions to sub-grids. Concentrations are then recalculated at the sub-grid level, using a Gaussian model, whilst removing the local contribution of the CTM at these sub-grids but keeping the non-local contributions. This procedure consistently avoids double counting of emissions.

Throughout this paper we refer to the downscaling grids in uEMEP as ‘sub-grids’. These may be any size but current applications use a range of between 25 and 250 m. When referring to the EMEP MSC-W model we use the term ‘grid’. This may also vary dependent on the application but is usually in the range of 2 to 15 km. The term ‘local’ is also used. Local, in regard to EMEP, means the local EMEP grids, so terms such as ‘local fraction’ refer to a particular grid and the other EMEP grids in the ‘local region’, for example within a range of 5 x 5 EMEP grids. When referring to ‘local’ in uEMEP we also refer to sub-grid contributions from within this local EMEP region. This is visualised in Fig. 1. ‘Non-local’, in regard to uEMEP, refers to any contribution that is not downscaled or calculated with uEMEP, usually contributions from outside the local EMEP region but these can also be other source sectors not accounted for by uEMEP. We will refer to concentrations provided by the EMEP MSC-W model simply as EMEP concentrations.

uEMEP can be run using two downscaling methods, both of which make use of Gaussian dispersion modelling to describe the redistribution of concentrations at high resolution. Both methods make use of the recently developed ‘local fraction’ functionality in the EMEP model (Sect. 2.3; Wind et al., 2020) to avoid double counting of emissions and to allow near seamless integration of the two models. The two downscaling methods are:

1. **Emission redistribution:** Redistribution of the EMEP gridded emissions using emission proxy data to sub-grids and calculation of concentrations through Gaussian modelling, with removal of the locally emitted EMEP concentrations.
2. **Independent emissions:** Independent high resolution emission data on sub-grids and calculation of the concentrations through Gaussian modelling, with removal of the locally emitted EMEP source contributions. **The independent emissions do not need to be consistent with the EMEP gridded emissions in this case.**

In addition calculations can be made on either long term mean emissions, using a rotationally symmetric dispersion kernel (Sect. 3.2), or on hourly emissions, using a slender plume Gaussian dispersion model (Sect. 3.1).

Typical source sectors downscaled using uEMEP include traffic, residential combustion, shipping and industry. The sectors addressed will depend on the availability of high resolution data for distributing them. uEMEP is only applied to the primary emissions of PM₁₀, PM_{2.5} and NO_x and does not involve any complex chemistry or secondary formation of particles. The concentrations of NO₂ and O₃ are calculated with uEMEP using a simplified chemistry scheme (Sect. 3.4 and 3.5).

2.2 Sub-grid calculation method

The choice of downscaling method will depend on the quality of the high resolution proxy or emission data available, whether the calculation will be made on hourly or annual data and on the EMEP model resolution. The first downscaling method, emission redistribution, will be applied when only approximate proxy data for emissions are available, which will be the case in many large scale applications. Examples of such proxy data may be population density, road network data or land use data.

The second downscaling method, independent emissions, is suitable for when high quality emission data is available that is consistent between uEMEP and EMEP. When the gridded emission data is entirely consistent with the proxy data, i.e. the proxy data are given as emissions and are aggregated to the CTM grid emissions, then the two methods are equivalent.

The total sub-grid concentrations $C_{SG}(i,j)$ at sub-grid indexes (i,j) are calculated by adding the local Gaussian concentration $C_{SG,local}(i,j)$ and the non-local part of the EMEP grid concentration $C_{SG,nonlocal}(i,j)$ and is written simply as

$$C_{SG}(i,j) = C_{SG,local}(i,j) + C_{SG,nonlocal}(i,j) \quad (1)$$

where we use the subscript notation 'SG' to denote any sub-grid value and in further equations the subscript 'G' to indicate any EMEP grid value. $C_{SG,local}(i,j)$ is determined directly from the sub-grid dispersion calculation

$$C_{SG,local}(i,j) = \sum_{i'=1}^{n_x} \sum_{j'=1}^{n_y} \frac{E_{SG,local}(i',j')}{U(i,j,i',j')} \cdot I(r(i,j,i',j'), h(i',j'), z(i,j)) \quad (2)$$

Here $E_{SG,local}$ is the emission attributed to each sub-grid and U is the wind speed, which in uEMEP is dependent on both the source and receptor sub-grid values (Sect. 3.1). n_x and n_y represent the extent of the sub-grid calculation window. The function $I(r,h,z)$ is the dispersion intensity function (Sect. 3.1) that determines the dispersion of the emission source $E_{SG,local}$ with the horizontal spatial vector $r(i,j,i',j')$ between the receptor grid points (i,j) and the source grid points (i',j') at height $z(i,j)$. The source height $h(i',j')$ is also specified. The contribution from every proxy emission sub-grid (i',j') , within the defined sub-grid calculation window (n_x, n_y) is calculated and summed at the receptor sub-grid (i,j) centered within sub-grid calculation window, see Fig. 1.

When using the emission redistribution method, $E_{SG,local}$ is calculated using the EMEP grid emissions $E_G(I,J)$ and the proxy data for emissions, $P_{emission}$. $P_{emission}$ is normalised within the EMEP grid in the following way to determine the sub-grid emission $E_{SG,local}$

$$E_{SG,local}(i',j') = E_G(I,J) \frac{P_{emission}(i',j')}{\sum_{i'=1}^{n_x} \sum_{j'=1}^{n_y} P_{emission}(i',j')} \quad (3)$$

When using the independent emission method, the local sub-grid emissions $E_{SG,local}$ are specified directly.

140 2.3 Calculation of the non-local contribution from EMEP

The term $C_{SG,nonlocal}(i,j)$ given in Eq. (1) and further derived in Eq. (9) and Eq. (10), is the non-local contribution from the EMEP grid at the specific sub-grid (i,j) . Though this is based on the non-local contribution provided by EMEP at grids (I,J) interpolation due to the moving window (Sect. 2.4) surrounding each receptor sub-grid means that non-local contributions are specified at the sub-grid level. The gridded non-local contribution, $C_{G,nonlocal}(I,J)$, is derived from the ‘local fraction’ calculation in EMEP. The methodology is described completely in Wind et al. (2020) but the essential elements are reproduced here.

The local fraction methodology corresponds to a tagging method, where pollutants from different origins are tagged and stored individually. In this case the tagging occurs relative to the surrounding grid cells of any individual grid. This means that emissions from any grid cell are tagged and followed through the various model processes out to neighbouring grid cells. Tagged species are assumed to be inert species, primary PM and NO_x , for this downscaling application as chemical reactions are not included in the tagging. It is generally not computationally possible, or in this application necessary, to follow all grid cell contributions to all other grids within the EMEP model domain. The local fraction region extent is then limited. In Wind et al. (2020) the local fraction region extent (n_{lf}) was tested up to a 161 x 161 EMEP grids on low resolution EMEP runs for Europe. Generally 21 x 21 EMEP grids were found to be computationally and memory efficient. In the uEMEP application the local fraction region needs only be as large as the uEMEP calculation window, i.e. the allowed distance from the receptor

sub-grid to the emission sub-grids. In the forecasting application discussed in Sect. 4 this requires only a 5 x 5 EMEP grid local fraction region. Sensitivity to the size of this region is discussed in Sect. S5.2. For each EMEP grid (I,J) there will be an associated local fraction grid $LF(I,J,I_{lf},J_{lf})$ that specifies the fraction of the surrounding grids contributing to the (I,J) grid. I_{lf} and J_{lf} are indexed from $-n_{lf}/2$ to $+n_{lf}/2$.

160

With use of the local fraction then the local ($C_{G,local}$) and non-local ($C_{G,nonlocal}$) contributions from any particular primary pollutant to an EMEP grid (I,J) is given by the sum of all the contributing local fraction contributions of the local sources ($s = I$ to n_{source}) and the non-local contribution, specified by

165

$$C_{G,local}(I,J,I_{lf},J_{lf},s) = LF(I,J,I_{lf},J_{lf},s) C_G(I,J) \quad (4)$$

$$C_{G,nonlocal}(I,J) = C_G(I,J) - \left\{ \sum_{I'=-n_{mw}/2}^{+n_{mw}/2} \sum_{J'=-n_{mw}/2}^{+n_{mw}/2} \sum_{s=1}^{n_{source}} C_{G,local}(I,J,I',J',s) \right\} \quad (5)$$

Note that in Wind et al. (2020) $C_{G,local}$ and C_G are termed *LP* (local pollutant) and *TP* (total pollutant) respectively and the local fraction index is specified here using (I_{lf},J_{lf}) instead of $(\Delta x_s, \Delta y_s)$ This change is for compatibility with the notation used for the uEMEP application.

170

2.4 Moving window calculation of local and non-local EMEP contributions

When determining the local and non-local EMEP contribution at any uEMEP sub-grid receptor then a moving window methodology is applied. The aim of the moving window calculation is to represent as well as possible the local and non-local EMEP contributions at any one sub-grid, in effect creating an EMEP grid that is centred on the receptor sub-grid. The moving window is centred on the receptor sub-grid (i,j) and its size is specified by the number of EMEP grids it covers (n_{mw} , n_{mw}). The moving window region is the same as the uEMEP calculation window in extent, which is also defined by the number of sub-grids (n_x , n_y), Sect. 2.2. n_{mw} is given by the user but it must not be larger than the area covered by the EMEP local fraction region (n_{lf}), i.e. $n_{mw} \leq n_{lf} - 1$. Fig. 1 shows an example where $n_{lf} = 5$ and $n_{mw} = 4$.

180

Since we need to account for all source contributions from EMEP within the moving window and since the sub-grids are not centred in the middle of the EMEP grids then the local contribution from the EMEP grids for any particular source sector s can be written as

185

$$C_{G,local}(i,j,s) = \sum_{I'=-n_{mw}/2}^{+n_{mw}/2} \sum_{J'=-n_{mw}/2}^{+n_{mw}/2} C_{G,local}(I,J,I',J',s) \cdot w(i,j,I',J',s) \quad (6)$$

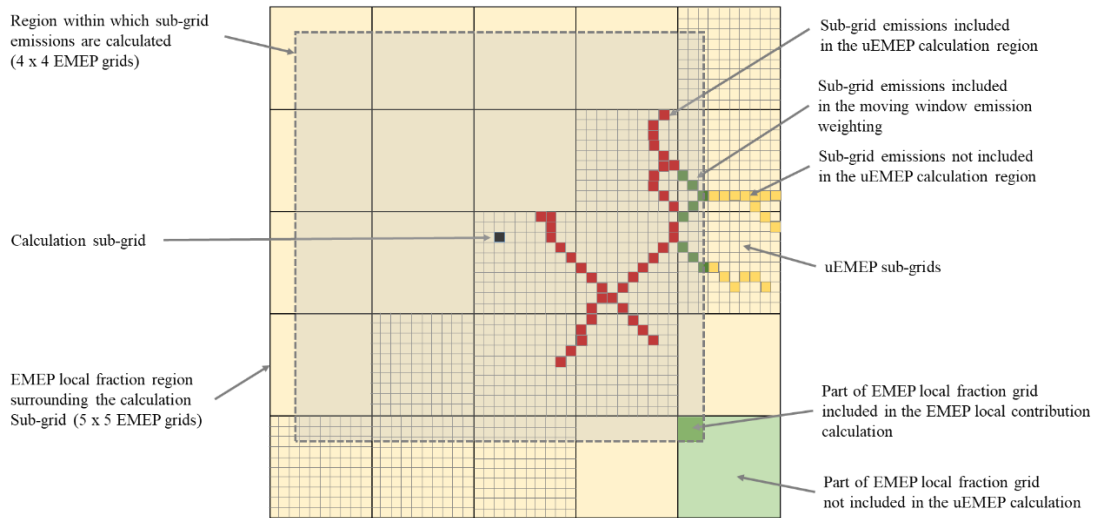
Here the weighting variable $w(i,j,I',J',s)$ refers to the weighting of the EMEP grid relative to the receptor sub-grid and the index I',J' refers to the EMEP grid which contains the uEMEP sub-grid (i,j) . For EMEP grids entirely within the moving window then this weighting will be unity, but for EMEP grids only partially within the moving window this weighting will be less than unity as part of that EMEP grid will also contribute to the non-local concentrations.

There are two methods implemented in uEMEP for specifying these weights. The simplest and most often used is area weighting where only the area fraction of the EMEP grid that is within the moving window for that particular receptor sub-grid is included in the local contribution. This is illustrated in Fig. 1 and is usually sufficient for the calculation, especially when the number of EMEP grids covered by the moving window is larger than 3×3 . Mathematically the area weighting, wa , can be written as

$$wa(i,j,I',J') = \frac{\{a(i,j) \cap A(I',J')\}}{A(I',J')} \quad (7)$$

where $A(I',J')$ is the area and position of each EMEP grid, $a(i,j)$ is the area and position of the moving window centred at the receptor sub-grid point (i,j) and $a(i,j) \cap A(I',J')$ is the overlapping area of these two regions. For the case where $n_{mw} = 1$ then this area weighting is equivalent to a bilinear interpolation of the surround EMEP grids. Area weighting is not dependent on the source.

Schematic representation of the uEMEP moving window region



205

Figure 1. Schematic representation of the moving window region. It shows the regions used for uEMEP calculations and the area and emission weighting selection used to determine the local and non-local EMEP contributions at the calculation (receptor) sub-grid. The extent of the sub-grids is only partially shown.

210

When the moving window only covers a limited number of EMEP grids and when high resolution emission data is used that is compatible with the EMEP grid emissions, then this weighting can also be based on the high resolution emission data itself. This better represents the moving window concept because it reflects the effect of moving the EMEP grid to be centred on the receptor sub-grid in a more realistic way. In this case the emission weighting term (we) on the edge of the moving window will be determined by the fraction of the total sub-grid emissions within the moving window and within the EMEP grid, instead of the area. This can be written as

215

$$we(i, j, I', J', s) = \frac{\sum e(i, j, I', J', s) : \in \{a(i, j) \cap A(I', J')\}}{\sum e(i, j, I', J', s) : \in \{A(I', J')\}} \quad (8)$$

220

where the numerator is the sum of the emissions within the intersection of $a(i, j)$ and $A(I', J')$ and the denominator is the sum of the emissions within $A(I', J')$. The resulting total concentration, using this method, may be higher or lower than the original EMEP concentrations because it reflects the impact of moving the EMEP grid in space. This is easiest to visualise if the moving window is the same size as the EMEP grid. If the moving window were centred on an area with concentrated emissions, that are in reality spread over two EMEP grids, then when using the emission weighting the new EMEP local contribution would be higher, the non-local lower and the total would be different, see Fig. 2. The opposite is also true if the moving window were placed over a region with low emissions, the local contribution would be lower and the non-local higher. Due to this, it is not possible simply to subtract the local EMEP contribution from the total to get the non-local EMEP contribution, as detailed in Eq. 5.

225

230

To address this the non-local EMEP contribution is also calculated using the moving window with Eq. (9). The first term is the non-local contribution for a particular source and is calculated with the area weighting distribution since non-local contributions, those outside the local fraction region, do not have any associated emission or local fraction for weighting. An additional correction term, second term in Eq. (9), accounts for the non-local contributions from local contributions on the EMEP edge grids, those parts of the EMEP grids that are outside the moving window and not included as a local contribution in Eq. 6. In those cases the local EMEP contribution outside the moving window must be converted to a non-local contribution and subtracted from the calculated non-local value, first term in Eq. 9.

235

$$C_{G,nonlocal}(i, j, s) = \sum_{I'=I-n_{mw}/2}^{I+n_{mw}/2} \sum_{J'=J-n_{mw}/2}^{J+n_{mw}/2} C_{G,nonlocal}(I', J', s) \cdot wa(i, j, I', J') - \sum_{I'=-n_{mw}/2}^{+n_{mw}/2} (I' \neq 0) \sum_{J'=-n_{mw}/2}^{+n_{mw}/2} (J' \neq 0) \left(C_{G,local}(I, J, I' \rightarrow I, J' \rightarrow J, s) \cdot w(i, j, I', J', s) \right) + C_{G,local}(I, J, I \rightarrow I', J \rightarrow J', s) \cdot w(i, j, I, J, s) \quad (9)$$

240

In Eq. (9) the weighting term w represents either the emission (we) or the area (wa) weighting, depending on the choice of weighting method.

245 These local and non-local calculations are carried out for each emission source individually so the non-local contribution is also dependent on source and the non-local component for any particular source will also contain the local contributions from the other sources. This makes creating a final non-local contribution complicated. To solve this, all the source specific $C_{G,local} + C_{G,nonlocal}$ contributions are averaged and the sum of the $C_{G,local}$ source contributions are subtracted to obtain the final $C_{G,nonlocal}$. The final non-local contribution at each sub-grid $C_{SG,nonlocal}$, Eq. (1), is equivalent to the EMEP non-local $C_{G,nonlocal}$ contribution and is calculated by

250

$$C_{SG,nonlocal}(i, j) = \frac{1}{n_{source}} \sum_{s=1}^{n_{source}} \{ (C_{G,local}(i, j, s) + C_{G,nonlocal}(i, j, s)) \} - \sum_{s=1}^{n_{source}} \{ C_{G,local}(i, j, s) \} \quad (10)$$

In the case of area weighting, where the sum of local and non-local is the same as the original EMEP total concentration, then the first term in the summation is equivalent to the original EMEP concentration without summation. The method is illustrated
255 in one dimension in Fig. 2.

The calculation based on emission weighting is computationally more expensive than the area weighting and is only used when necessary and appropriate, e.g. when $n_{mw} = 1$ and when sub-grid and grid emissions are consistent with each other.

260

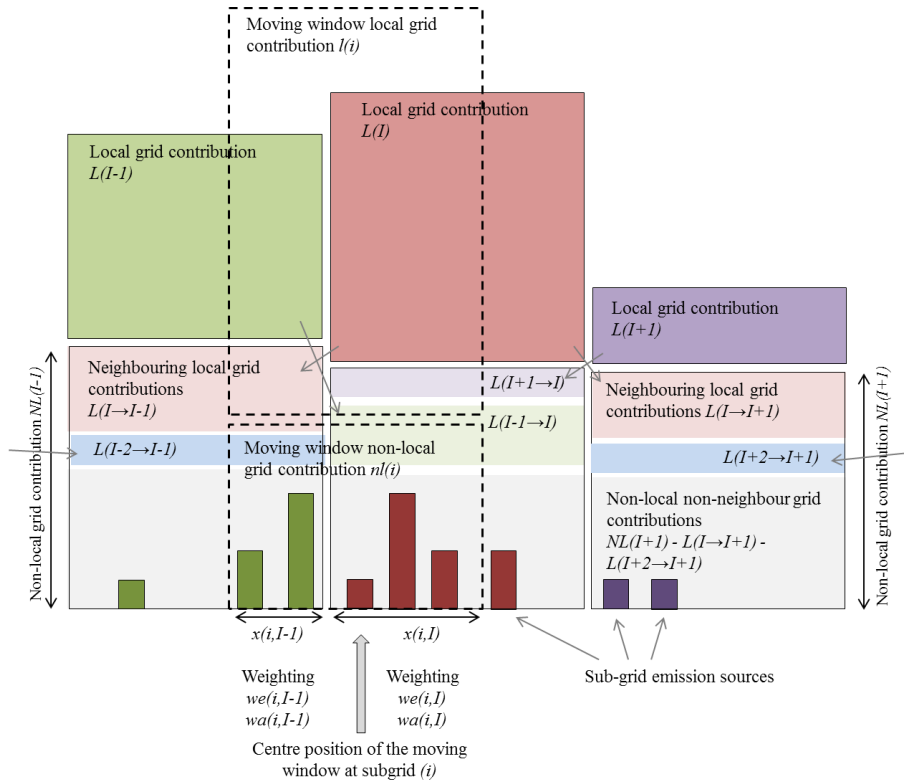


Figure 2. Illustration of the moving window interpolation method employed in uEMEP. Shown is the 1D visualisation of the 2D method described in Eq. 6 - 10 for $n_{mw} = 1$. For clarity in the figure the terms $C_{G,local}$ and $C_{Gnonlocal}$ are written as L and NL respectively.

265 3. uEMEP model process description and parameterisation

In this section uEMEP process parameterisations are described. In regard to the dispersion modelling uEMEP is intended to integrate closely with EMEP. To enable this, dispersion schemes based on parameterisations used in EMEP have been implemented. In the supplementary material additional equations (Sect. S1-S3) are provided and a number of optional additional parameterisations are also described (Sect. S4).

270 3.1 Sub-grid Gaussian dispersion modelling for hourly calculations

A standard Gaussian narrow plume dispersion model formulation, e.g. Seinfeld and Pandis (1998), is used in the sub-grid dispersion calculations with multiple reflections from the surface ($z=0$) and boundary layer height ($z=H$). Generically the Gaussian plume calculation can be written as

$$275 \quad C(x, y, z) = \frac{Q}{u} I(x, y, z) \quad (11)$$

where for the sake of clarity we have dropped references to sub-grid indexes as given in Sect. 2 and use coordinates instead of indices. Here C is the concentration, Q is the emission source strength and I is the plume intensity given by

$$280 \quad I(x, y, z) = \frac{1}{2\pi\sigma_y\sigma_z} \exp\left(\frac{-y^2}{2\sigma_y^2}\right) \sum_{i=1}^{i=6} \left\{ \exp\left(\frac{-(z-h_i)^2}{2\sigma_z^2}\right) \right\} \quad (12)$$

Here h_i represents the plume emission height and five additional virtual plume emission heights after single and double reflections from the surface and boundary layer top (H) given by

$$285 \quad h_i = [h_{emis}, -h_{emis}, 2H - h_{emis}, 2H + h_{emis}, -2H + h_{emis}, -2H - h_{emis}] \quad (13)$$

For the well mixed plume case, when σ_z is of the order of H , we define a threshold beyond which the plume concentration is constant throughout the boundary layer. This is specified to occur when $\sigma_z > 0.9H$ leading to an intensity given by

$$290 \quad I(x, y, z) = \frac{1}{\sqrt{2\pi}\sigma_y H} \exp\left(\frac{-y^2}{2\sigma_y^2}\right) \quad (14)$$

The Gaussian dispersion parameters σ_z and σ_y used in Eq. (12) may be determined empirically (Smith, 1973; Martin, 1976; Turner, 1994; Liu et al., 2015) or through a range of methods based on theoretical and semi-empirical considerations (Seinfeld and Pandis, 1998). Venkatram (1996) also discusses the relationship between empirically and theoretically based dispersion
 295 parameters. Standard Gaussian plume models do not take into account variable vertical profiles of wind speed or diffusivity. Some non-Gaussian descriptions are available based on the application of power laws to these profiles and the vertical integration of the diffusion equation (Chaudhry and Meroney, 1973; van Ulden, 1978; Venkatram et al., 2013) but this then creates the problem of defining power laws that ‘fit’ varying wind and dispersion profiles over the entire boundary layer. Instead of this we use the center of mass of the plume (z_{cm}) to define the height at which the advective wind speed and eddy
 300 diffusivity (K_z) are defined and allow this to vary dependent on the plume travel distance, giving a similar effect to the plume dispersion as the non-Gaussian vertically integrated derivation. A similar methodology is employed by the OPS model (Sauter et al, 2018). We then use a combination of eddy diffusivity (K_z) vertical profiles, Lagrangian time scales and centre of mass plume placement, along with initial values σ_{z0} and σ_{y0} , to determine σ_z and σ_y values. The aim of this combination is to provide realistic plume dispersion over short distances but to asymptotically approach the same K_z values used in the EMEP model
 305 dispersion scheme over longer distances. In addition the methodology is implementable at all emission heights and takes into account both surface roughness and atmospheric boundary layer height.

Following methodologies outlined in Seinfeld and Pandis (1998), we describe the dispersion parameters σ_z and σ_y as a function of pollutant travel time from source (t) using

310

$$\sigma_z(t) = \sigma_{z0} + \sqrt{2K_z(z)t f_t} \quad (15a)$$

$$\sigma_y(t) = \sigma_{y0} + \sqrt{2K_y(z)t f_t} \quad (15b)$$

where σ_{z0} and σ_{y0} are initial dispersion parameters, $K_z(z)$ and $K_y(z)$ are the vertical profiles of vertical and horizontal eddy diffusivity and f_t is a factor dependent on the Lagrangian integral time scale τ_l given by

315

$$f_t = 1 + \left(\frac{\tau_l}{t} \exp\left(-\frac{t}{\tau_l}\right) - 1 \right) \quad (16)$$

There are many varying methods for calculating the Lagrangian integral time scale (Seinfeld and Pandis, 1998; Hanna, 1981; Venkatram, 1984). We use the formulation from Hanna (1981)

320

$$\tau_l = 0.6 \frac{\max(z_{emis}, z_{\tau min})}{u_*} \quad (17)$$

where z_{emis} is the emission height, u_* is the friction velocity and $z_{\tau min} = 2m$. Time is calculated from the advective velocity

325

$$t = \frac{\max(x_{min}, x)}{U(z)} \quad (18)$$

where x_{min} is half a sub-grid, $U(z)$ is the vertical wind speed profile and x is the down plume distance.

In order to be compatible with the EMEP model the same K_z vertical profile parameterization is used in Eq. (15a) that is used in EMEP (Simpson et al., 2012). This parameterization is provided in the supplementary material, Eq. (S1-S2).

The center of mass of the plume is calculated using the same Gaussian formulation with reflection as given in Eq. (12) by integrating the plume intensity over the boundary layer height (H) using

335

$$z_{cm} = \frac{\int_0^H z I(z) dz}{\int_0^H I(z) dz} \quad (19)$$

This integral can be analytically solved to give

340
$$z_{cm} = \frac{\sigma_z}{\sqrt{2\pi}} \sum_{i=1}^{i=6} \exp\left(\frac{-h_i^2}{2\sigma_z^2}\right) - \exp\left(\frac{-(H-h_i)^2}{2\sigma_z^2}\right) + \frac{h_i}{2} \left(\operatorname{erf}\left(\frac{h_i}{\sqrt{2}\sigma_z}\right) + \operatorname{erf}\left(\frac{(H-h_i)}{\sqrt{2}\sigma_z}\right) \right) \quad (20)$$

and for the well mixed case where

$$\sigma_z > 0.9H \text{ then } z_{cm} = 0.5 H \quad (21)$$

345

The vertical wind profile is calculated in a similar way to Gryning et al. (2007), based on decreasing turbulent shear with height.

$$U(z) = \frac{u_{*0}}{\kappa} \left(\log\left(\frac{z}{z_0}\right) - \psi_m + \kappa \frac{z}{z_l} \left(1 - \frac{z}{2H}\right) - \frac{z}{H} \left(1 + b \frac{z}{2L}\right) \right) \text{ for } L \geq 0$$

350
$$U(z) = \frac{u_{*0}}{\kappa} \left(\log\left(\frac{z}{z_0}\right) - \psi_m + \kappa \frac{z}{z_l} \left(1 - \frac{z}{2H}\right) - \frac{z}{H} \frac{((a z - L)\phi_m + L)}{a(p+1)} \right) \text{ for } L < 0 \quad (22)$$

The stability functions ψ_m and ϕ_m are defined in the supplementary material, Eq. (S3-S4), and the assumptions behind the wind profile derivation are given in Eq. (S5-S8). There is no turning of the wind direction with height. Eq. (22) is used to derive u_{*0} , based on modelled 10 m wind speed, boundary layer height H, **Monin-Obukhov length (L)** and surface roughness length z_0 .

355 The vertical wind profile is then derived from this. **A minimum wind speed of 0.5 m/s for all dispersion calculations has been imposed.**

The average of the plume center of mass height at the receptor point and the emission height, $z_{av} = 0.5 (z_{cm} + h_{emis})$, is then used to determine the vertical diffusion $K_z(z_{av})$ as well as the wind speed $U(z_{av})$ for use in Eq. (15) and (18). The entire set of
360 equations, Eq. (15-22) are solved iteratively to obtain the final σ_z value at the receptor point. This iteration converges swiftly and generally only two iterations are required.

The horizontal eddy diffusivity K_y is not determined in EMEP so an alternative is required. K_y can be classically related to K_z through the relationship

365

$$K_y(z) = \frac{\sigma_v(z)^2}{\sigma_w(z)^2} K_z(z) \quad (23)$$

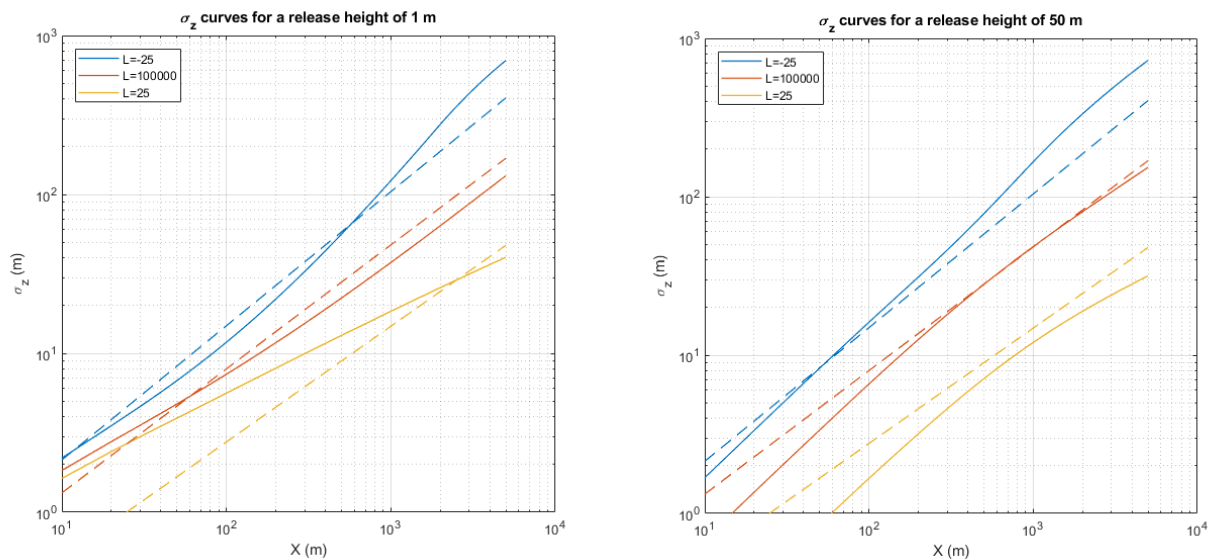
based on the concepts used to define K (Seinfeld and Pandis, 1998). Garratt (1994) provides expressions for the vertical profile σ_v and σ_w under unstable conditions where the ratio σ_v/σ_w is around 1.85 in the surface layer but decreases to 1 in the mixed

370 layer. Under stable conditions Nieuwstadt (1984) provides local scaling where this ratio is close to 2. For the current application we choose the ratio $\sigma_v/\sigma_w = 2$ and apply it over the whole boundary layer.

It is also possible within the modelling setup to use the simpler empirical formulations of σ_z and σ_y , as presented in Eq. (24) and shown in Table 1. This is useful for testing and comparison and necessary when using the rotationally symmetric plume parameterization, Sect. 3.2. See Seinfeld and Pandis (1998) for a presentation of these.

In Figure 3 we show two example sets of σ_z curves for near surface (1 m) and elevated (50 m) releases as calculated with the K_z methodology for three separate stabilities. For reference the dispersion curves from ASME (American Society of Mechanical Engineers), Smith (1973) are also shown. These often used dispersion parameters are relevant for one hour averaging times. The ASME σ_z curves are given in Pasquill stability classes and the conversion from their dependency on L and z_0 is achieved using the conversion methodology described by Golder (1972). Parameters used in the calculation of the 3 curves are provided in Table 1.

In addition to the parameterizations presented here uEMEP also includes parameterizations, provided in the supplementary material, for plume meandering and change of wind direction (Sect. S3.4.1), traffic induced initial dispersion (Sect. S3.4.3) and road tunnel internal deposition and emissions (Sect. S3.4.5).



390 **Figure 3. Comparison of derived σ_z curves discussed in the text with standard ASME curves (Smith, 1973) using Eq. (24). To the left a 1 m release and to the right a 50 m release. Three different stability classes, specified by the Monin–Obukhov lengths (L), are shown. The K_z method is shown as a solid line and the ASME curves as dashed lines. The ASME curves have no release height or surface roughness dependence but are included as reference. Values of $z_0=0.5$ m, relevant for urban areas, and $\sigma_{z0} = 0$ are used.**

Table 1. Parameters used for calculating the curves shown in Fig. 3.

Stability	z_0 (m)	H (m)	L (m)	ASME a_z	ASME b_z
Unstable	0.5	2000	-25	0.401	0.844
Neutral	0.5	1000	+100000	0.22	0.780
Stable	0.5	100	+25	0.097	0.728

395 **3.2 Rotationally symmetric Gaussian plume model for annual mean calculations**

When applying uEMEP to annual mean emissions a rotationally symmetric Gaussian plume is used. It is possible to derive an approximate analytical solution to the Gaussian plume equation assuming that wind directions are homogeneously distributed in all directions and that there is no strong dependence of wind speed or stability on wind direction. These conditions are usually not met but it is useful to have such a simplified analytical solution.

400

The starting point is the Gaussian plume model given in Eq. (12). In this case we do not derive $\sigma_{y,z}$ using the K_z value from EMEP but apply the commonly used power law formulation in order to derive an analytical solution

$$\sigma_{(y,z)} = \sigma_{0(y,z)} + a_{(y,z)} x^{b(y,z)} \quad (24)$$

405

Values for the dispersion parameters a and b may be taken from the literature (Seinfeld and Pandis, 1998) but we use the ASME curves (Smith, 1973) under neutral conditions to specify these.

The rotationally symmetric version of this equation can be derived by rewriting the equation in cylindrical coordinates with appropriate approximations (second order), based on the slender plume assumption, and integrating over all angles. The resulting rotationally symmetric intensity $I_{rot}(r,z)$ as a function of r and z is then written

410

$$I_{rot}(r,z) = \frac{1}{\pi\sqrt{2\pi r \varepsilon_z \sqrt{1+B}}} \operatorname{erf} \left(\frac{\pi\sqrt{1+B}}{\sqrt{2}\varepsilon_\theta} \right) \sum_{i=1}^{i=6} \left\{ \exp \left(\frac{-(z-h_i)^2}{2\varepsilon_z^2} \right) \right\} \quad (25)$$

415 where

$$\varepsilon_z = \sigma_{0z} + a_z r^{b_z} \quad (26a)$$

$$\varepsilon_\theta = \frac{1}{r} (\sigma_{0y} + a_y r^{b_y}) \quad (26b)$$

$$B = -\varepsilon_\theta^2 \left(\frac{b_z(\varepsilon_z - \sigma_{0z})}{r\varepsilon_\theta} + \frac{b_y(r\varepsilon_\theta - \sigma_{0y})}{\varepsilon_z} \right) \quad (26c)$$

420

The term B can be less than -1, typically when $r < 2\sigma_{0,y}$, which can lead to imaginary solutions. This is due to the second order approximation made in converting to cylindrical coordinates. In that case we write a second order approximation based on Taylor series expansion around $B = -1$ as

$$I_{rot}(r, z) = \frac{1}{2\pi r \varepsilon_z \varepsilon_\theta} \left(1 - \frac{\pi^2(1+B)}{6\varepsilon_\theta^2} + \frac{\pi^4(1+B)^2}{40\varepsilon_\theta^4} \right) \sum_{i=1}^{i=6} \left\{ \exp\left(\frac{-(z-h_i)^2}{2\varepsilon_z^2}\right) \right\} \quad \text{for } B < -1 \quad (27)$$

A similar derivation has been carried out by Green (1980) using different assumptions for the form of Eq. (24).

3.3 Initial dispersion

In Sect. 3.1 and 3.2 the hourly and annual dispersion parameterizations are described. In both cases initial values for $\sigma_{0(y,z)}$ are required. Since we treat the sources as small area emitters we set the initial σ_{0y} to correspond to these areas. A value of $\sigma_{0y} = \Delta y / \sqrt{2\pi} \approx 0.8 (\Delta y / 2)$ will give a maximum sub-grid center concentration equivalent to the concentration that would be found if the emissions were distributed evenly in the sub-grid. We then write the total initial dispersion to be

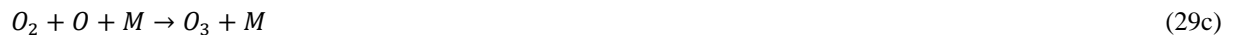
$$\sigma_{0y} = \sigma_{init,y} + 0.8 \frac{\Delta y}{2} \quad (28)$$

In all applications of uEMEP $\Delta x = \Delta y$. The other parameter, $\sigma_{init,y}$, is a specific initial dispersion width for each individual emission source, for example 2 m for **traffic** and 5 m for **shipping, heating and industry**. This is generally much smaller than the emissions grids.

The initial value for σ_{0z} is also a combination of a specific emission initial dispersion, for example $\sigma_{init,z} = 5$ m for residential wood combustion, but also uses the displacement technique for the plume where the start of the plume is displaced upwind by $\Delta x / 2$ allowing the plume to grow vertically over half the sub-grid distance. Tunnel exits are given an initial $\sigma_{init,z} = 6$ m to represent the extended size of the tunnel portals.

3.4 NO₂ chemistry for hourly means

The only chemistry included in uEMEP is the NO_x, O₃ chemical reactions. We use a similar methodology to Benson (1984, 1992) known as the discrete parcel method but use a weighted time scale over which the reactions take place. The following chemical reactions are involved, with O_x (O₃+NO₂) and NO_x (NO+NO₂) concentrations being conserved:



Eq. (29c) occurs on time scales much faster than the two other reactions and is taken to be instantaneous. The differential equation for the concentration of $[NO_2]$ as a function of time is written as

455

$$\frac{d[NO_2]}{dt} = k_1[NO][O_3] - J[NO_2] \quad (30)$$

where the concentrations are expressed in terms of molecules/cm³ and J is the photolysis rate (s^{-1}) for Eq. (29b) taken from the EMEP model (Simpson et al., 2012). The reaction rate k_1 for Eq. (29a) is given by

460

$$k_1 = 1.4 \times 10^{-12} \exp\left(\frac{-1310}{T_{air}}\right) \text{ (cm}^3\text{s}^{-1}\text{)} \quad (31)$$

as in the EMEP model and where T_{air} is in the atmospheric temperature (K).

465 We rewrite Eq. (30) in terms of the dimensionless ratios

$$f_{NO2} = \frac{[NO_2]}{[NO_x]} \text{ and } f_{Ox} = \frac{[O_x]}{[NO_x]} \quad (32a)$$

$$J' = \frac{J}{k_1[NO_x]} \quad (32b)$$

$$t' = tk_1[NO_x] \quad (32c)$$

470

Eq. (30) then becomes

$$\frac{df_{NO2}}{dt'} = (1 - f_{NO2})(f_{Ox} - f_{NO2}) - J'f_{NO2} \quad (33)$$

475 The solution to this equation is

$$f_{NO2} = \frac{B(1 - A \exp(Bt'))}{2(1 + A \exp(Bt'))} + \frac{C}{2} \quad (34)$$

where

$$A = \frac{B+C-2f_{NO2,0}}{B-C+2f_{NO2,0}} \quad (35a)$$

$$B = \sqrt{C^2 - 4f_{Ox}} \quad (35b)$$

$$C = 1 + f_{O_x} + J' \quad (35c)$$

and $f_{NO_2,0}$ is the initial NO_2 fraction at time $t'=0$.

485

This solution is valid for a box model without dilution through dispersion since it does not take into account how changing NO_x and O_x concentrations over the plume travel time will affect the reaction rates. Though this could be accounted for when applied to a single source with assumed dilution rates, by adding a time dependent diluting term to Eq. (30), this is not practically possible for multiple sources of differing dilutions. The concentrations of NO_2 at the start of the plume will be correctly calculated but NO_2 concentrations further from the plume will be slightly underestimated, since they do not have the higher initial reaction rates. Eventually the concentrations will reach photo-stationary equilibrium and here too NO_2 will be correctly calculated. This special case for photo-stationary equilibrium in Eq. (35) occurs when $t' \rightarrow \infty$ and Eq. (34) becomes

490

$$f_{NO_2} = \frac{C-B}{2} \quad (36)$$

495

The non-linear nature of Eq. (34) also means that it cannot be consistently applied to Gaussian models since the shape of the plume will change due to the non-linearity. Despite this, this formulation is more physically realistic than the photo-stationary assumption often used in local scale air quality modelling or other less physical parameterizations based on empirical fits. See Denby (2011) for an overview of the various NO_2 chemistry parameterization methods used with Gaussian modelling.

500

In order to calculate Eq. (34) in the model application an initial NO_x and O_x concentration must be used and a travel time defined. For multiple sources this travel time will vary so for each calculated sub-grid concentration of NO_x from each contributing sub-grid source (n_s sources) a travel time, t_s , is calculated based on the distance and wind speed. This is weighted based on the contribution of each source to the total sub-grid NO_x concentration. This provides a final weighted travel time t_w that is applied in Eq. (34). This ensures that nearest of the contributing sub-grids, often with the highest contributing NO_x concentrations, are given a higher travel time weight. A minimum distance, and hence time, of half a sub-grid is applied when calculating travel times.

505

$$t_w = \frac{\sum_{s=1}^{n_s} t_s [NO_x]_s}{\sum_{s=1}^{n_s} [NO_x]_s} \quad (37)$$

510

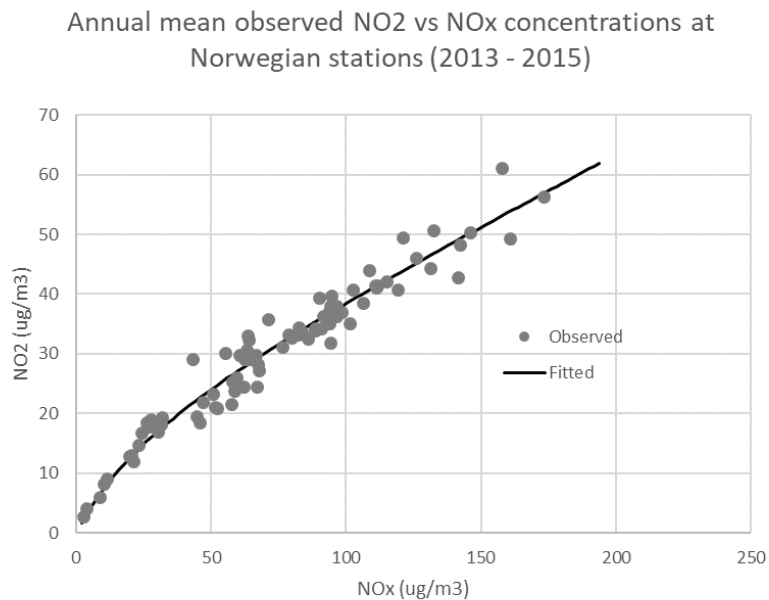
Comparisons with EMEP NO_2 calculations show that this chemistry scheme matches the results obtained by EMEP over longer time periods.

3.5 NO₂ – NO_x conversion for annual means

515 When annual mean data are used then the hourly mean formulation cannot be applied. Instead we use an empirically based conversion of NO_x to NO₂ based on the type of formulation from Romberg (1996) and updated by Bächlin and Bösinger (2008). 3 years of Norwegian NO₂ measurements, 82 measurements in all, have been used to determine this relationship, Fig. 5.

520
$$[NO_2] = \frac{a [NO_x]}{[NO_x]+b} + c [NO_x] \quad (38)$$

The fitted constants are determined to be a=20, b=30 and c=0.23. The estimated uncertainty in this conversion is around 10%, based on the normalized root mean square error of the fitted and observed NO₂ concentrations.



525 **Figure 5. NO₂ versus NO_x annual mean concentrations for all stations in Norway in the period 2013-2015. The fitted curve is based on Eq. (38).**

This empirical relationship will vary from region to region, largely due to differences in O₃ concentrations and photolysis rates that are not included as part of the parameterization. If used over large regions, for example Europe, then the uncertainty in the NO₂ conversion will increase.

530 3.6 Implementation

3.6.1 Sub-grid domains

Within uEMEP individual domains are defined with differing resolutions and sizes, dependent on which modelling parameter is represented. Separate domains and sub-grid resolutions are defined for each of the emission sources, for the time profiles of each emission sources, for the meteorological data, for the population data and for the receptor sub-grid concentrations. None
535 of these are required to have the same resolution or size, however, the highest resolution emission sub-grid will define the receptor sub-grid resolution, since there is no need to calculate on higher resolution sub-grids than is provided by the emissions. For emission sub-grids with lower resolution than the final receptor sub-grid domain then the dispersion calculations are first carried out at the same resolution as the emission domain and then bilinearly interpolated to the receptor sub-grid. For most urban applications this means that the choice of traffic sub-grid resolution defines the highest resolution sub-grid.

540

Emission sub-grids also contain properties for the dispersion calculations, such as initial dispersion parameters and emission heights. Each emission sub-grid has only one emission height h_{emis} , one $\sigma_{init,z0}$ and one $\sigma_{init,y0}$ for each emission source type. When multiple emissions from the same source type are placed in an emission sub-grid then the emission parameters are weighted by each individual emission. This is most relevant for industrial emissions which may have different emission heights
545 from separate stacks within a single emission sub-grid.

3.6.2 Selective sub-grid calculations

uEMEP does not necessarily calculate concentrations at all receptor sub-grids. Only sub-grids which are within $3\sigma_y$ of a plume centre line will be calculated and also downwind selection is used (Supplementary material, Sect. S3.4.2). In addition, a number of selections can be made allowing quicker calculations for particular applications. These include:

- 550 1. Calculation at defined receptor points, usually corresponding to measurement stations. In this case uEMEP calculates the surrounding 9 sub-grids and uses bilinear interpolation to extract the concentrations at the required receptor position.
2. Calculation at population grids. In this case concentrations will only be calculated at grids with non-zero population. This provides quicker exposure calculations than if the entire region was calculated
- 555 3. High density calculations near sources. A routine for selecting a higher density of sub-grids near sources may also be used to speed up calculations. This applies most often to traffic emission sub-grids that are near surface and with large gradients near the source. This is less useful for higher release sources as their maximum impact occurs further downwind than their emissions. After calculation the lower density receptor sub-grids are interpolated into the rest of the receptor sub-grids, providing a full receptor sub-grid domain

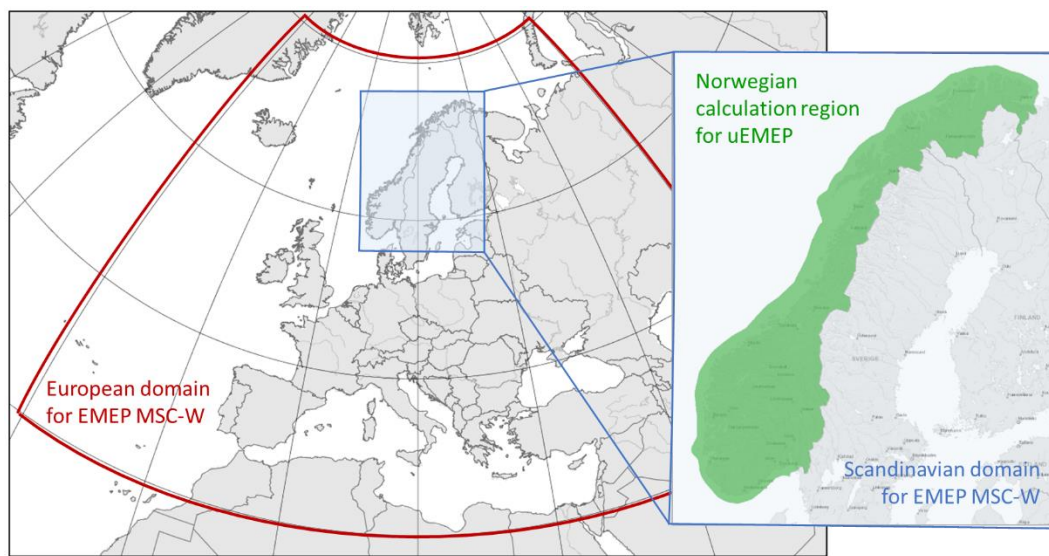
560 3.6.3 Model inputs and outputs

Input data comes from a variety of sources and the formatting of these sources varies. Emission input data is generally in text format whilst meteorological files are read from netcdf files.

565 Output of the model is in the form of netcdf files for either gridded data or point data, if receptor points have been defined. In both these files output includes the total concentrations of the pollutants along with the source contribution from each of the emission sources used in the calculation. Speciation of PM from EMEP can also be included in the output files, along with emissions, meteorology and population data.

4. Implementation in the Norwegian air quality forecast and analysis system

570 Though uEMEP has been applied in a number of applications we select the Norwegian forecast and analysis system (Norwegian air quality forecasting service, 2020) as an example. This application started operationally in the winter of 2018-2019 and provides daily forecasts of air quality for all of Norway two days in advance at sub-grid resolutions of between 250 and 50 m. In addition, the same system is used to calculate air quality retrospectively for analysis and planning applications (Norwegian air quality expert user service, 2020). The compounds PM_{2.5}, PM₁₀, NO₂, NO_x and O₃ are calculated. For each of these the local source contributions are determined separately for traffic exhaust, traffic non-exhaust, residential wood combustion, shipping and industry. A cascade of models are used starting with EMEP MSC-W at 0.1° European domain, EMEP MSC-W at 2.5 km Scandinavian domain and uEMEP 250-50 m Norway only, Fig. 6.



580 **Figure 6. Model domain for the European and Scandinavian EMEP MSC-W calculations and the uEMEP calculations**
(©kartverket/norgeskart.no).

4.1 Calculation steps

We describe below the implementation steps used in the Norwegian forecasting and analysis system. This implementation of
585 uEMEP uses the independent emission and replacement downscaling method (method 2 in Sect. 2). The following steps are
carried out:

1. High resolution emission data for Norway are calculated for each forecast (Sect. 4.2) and are aggregated into the EMEP MSC-W Scandinavian model grid. Some of these emissions require meteorological data.
2. The EMEP MSC-W model is used to calculate the large scale concentration distribution on an hourly basis, nesting
590 from a European domain ($\sim 0.1^\circ$) to the Scandinavian domain (2.5 km), Fig. 6. Within Norway the aggregated high
resolution aggregated emissions are implemented. Both EMEP calculations provide the local fraction (Sect. 2.3) in a
region of 5 x 5 EMEP grids.

The following three steps are then undertaken to calculate the uEMEP concentrations:

3. For the Norwegian forecast system the entire country is split into 1864 separate tiles of varying sizes and resolutions;
595 the resolution depending on the population and emission sources within each tile. Tiles with resolutions of 250 m can
be as large as 40 x 40 km² whilst tiles with resolutions of 50 m are no larger than 5 x 5 km². Tiling the calculations is
a form of external parallelisation and is optimised for both runtime and memory use. A two day forecast run on 196
processors takes roughly one hour of CPU time.
4. The high resolution emission data from the various source sectors (Sect. 4.2) is placed into the emission sub-grids in
600 uEMEP. These are between 50 – 250 m in width, depending on the emissions available and on the population density
of the region. Emission grid domains extend beyond the size of each tile so that the calculations are consistent over
tile borders.
5. uEMEP Gaussian dispersion modelling is applied (Sect. 3.1) using the sub-grid emissions as sources and the
concentrations are calculated at each sub-grid. Only sub-grid emissions within a region defined by a 4 x 4 EMEP grid
605 area are included in the sub-grid calculation, i.e. 10 x 10 km², corresponding to the extent of the moving window.
This 4 x 4 limit guarantees that the calculation will always be carried out within the EMEP 5 x 5 local fraction region.

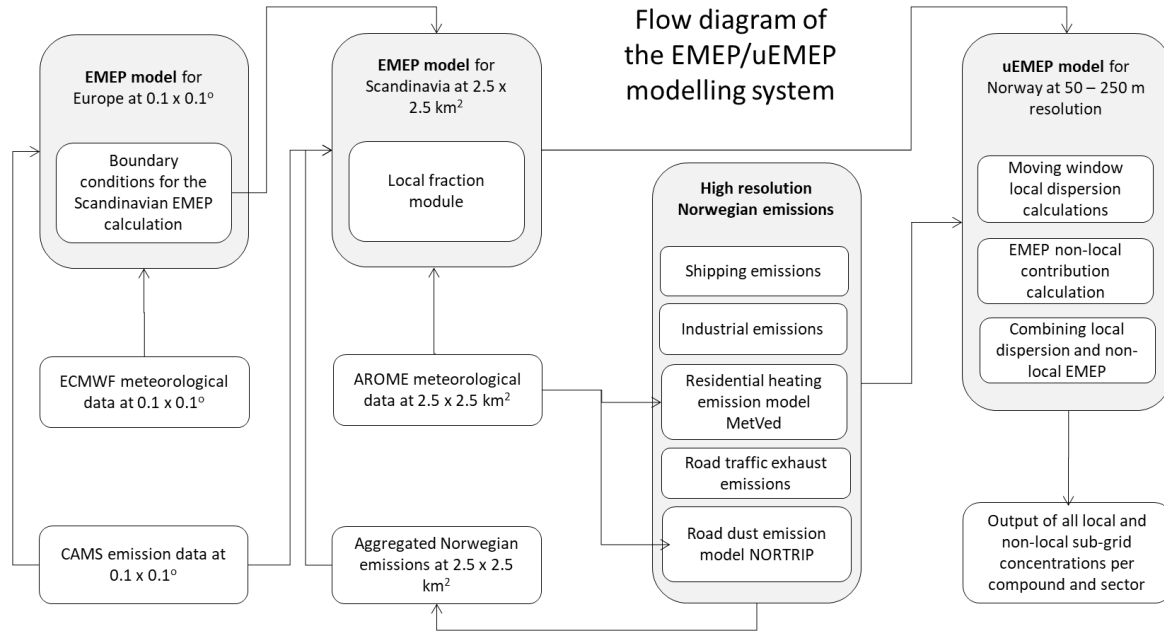
The final steps combine the EMEP gridded concentrations with the uEMEP sub-grid concentrations in the following way:

6. At each sub-grid the non-local contribution from the neighbouring 4 x 4 EMEP grids is calculated, Sect. 2.4. The
calculation is carried out for each source sector and each primary compound
- 610 7. The uEMEP calculations are then added to the non-local EMEP concentrations. In the case of PM then all non-primary
species are also added to the local and non-local EMEP primary concentrations
8. For NO₂ the chemistry (Sect. 3.4) is applied to determine NO₂ and ozone for each sub-grid

9. Sub-grid concentrations and their contributions are saved along with the PM speciation from EMEP in netcdf format.
10. The forecasts are made available to a public website through an API and Web Map Tile Server (Norwegian air quality forecasting service, 2020)

615

The system is schematically illustrated in Fig. 7. The following sections describe some steps in more detail.



620

Figure 7. Flow diagram showing the various components of the Norwegian EMEP/uEMEP forecast system.

4.2 Emissions

The EMEP calculations make use of the CAMS-REG-AP_v1.1 regional anthropogenic emission dataset everywhere in Europe (Kuenen et al., 2014; Granier et al., 2019). Only in the 2.5 km Scandinavian calculation, and only in Norway, are the emissions replaced with the aggregated high resolution dataset. The alternative emissions used in the calculations for Norway are:

625

- Road traffic exhaust emissions
- Road traffic non-exhaust emissions
- Residential wood combustion
- Shipping
- Industry

630

These emission sources are described in the supplementary material, Sect. S4.2. For other sectors the CAMS-REG-AP_v1.1 emissions are also used in Norway, but these emissions are not downscaled using uEMEP.

4.3 Meteorology

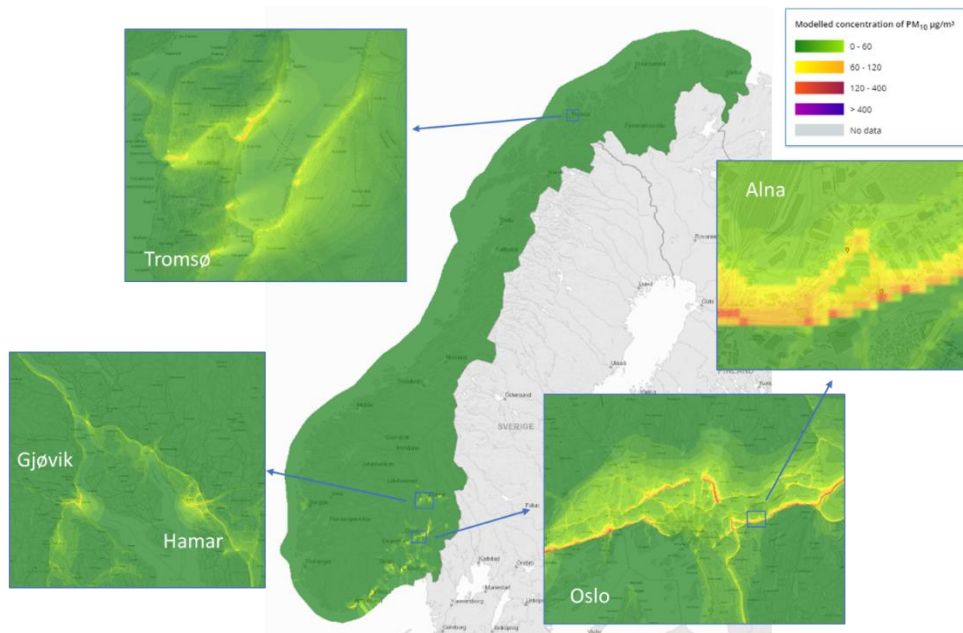
635 The meteorological forecast data used for the European EMEP model calculations is based on the Integrated Forecasting System (IFS, 2020) from the European Centre for Medium-Range Weather Forecasts (ECMWF, 2020). The Scandinavian EMEP model calculation uses the AROME-MetCoOp model for modelling meteorology over Scandinavia (Müller et al., 2017). This last model calculates meteorology at a resolution of 2.5 km and provides forecasts for 66 hours in advance. The EMEP MSC-W Scandinavian domain uses the same gridding and projection as the meteorological forecast model but in a
640 smaller domain.

4.4 EMEP MSC-W model implementation

The European EMEP MSC-W model calculation is based on the same daily forecast provided for the Copernicus Atmosphere Monitoring Service (CAMS, 2020; Tarrason, 2018) but is run independently and provides boundary conditions for the Scandinavian implementation of EMEP MSC-W at 2.5 km. The Scandinavian EMEP MSC-W calculation includes the
645 Norwegian emission sources described in Sect. 4.2 and also delivers the necessary local fraction information for use in uEMEP.

4.5 uEMEP model implementation

uEMEP calculates concentrations for all of Norway on grids with resolutions between 50 – 250 m using 1864 individual tiles as described in Sect. 4.1. The resolution of these tiles is defined by the population density and road density information. Tiles with higher population density use 50 m resolution, whilst tiles with lower population density but some traffic have a resolution
650 of 125 m. Tiles with very low traffic density but with shipping or wood burning emissions have a resolution of 250 m, corresponding to the emission resolution. Separate calculations are carried out at measurement sites, 72, with a sub-grid resolution of 25 m. An example of a PM_{10} forecast is shown in Fig. 8.



655 **Figure 8:** Example maps of PM_{10} concentrations taken from the forecast 24.02.2020 18:00 UTC. Resolution in populated city regions is 50 m. High PM_{10} concentrations along roads are mainly the result of road dust emissions (©kartverket/norgeskart.no).

5. Results

5.1 Validation against observations for the Norwegian forecasting and assessment system

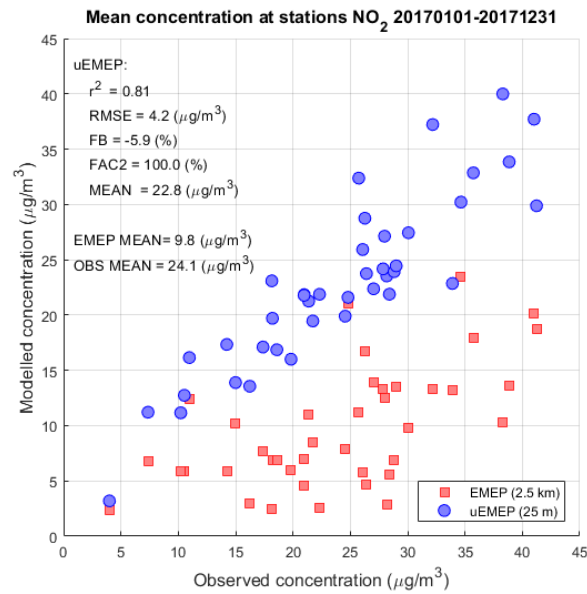
In the supplementary material we provide a complete and detailed statistical validation for the year 2017. Here we present a
 660 visual summary of results for NO_2 , PM_{10} and $PM_{2.5}$ for the same year. In 2017 there were 72 operational air quality stations. Not all stations measure all components so the total number of available stations for NO_2 and PM with coverage of more than 75% is between 34 – 45. The station positions are shown in Fig. 9.



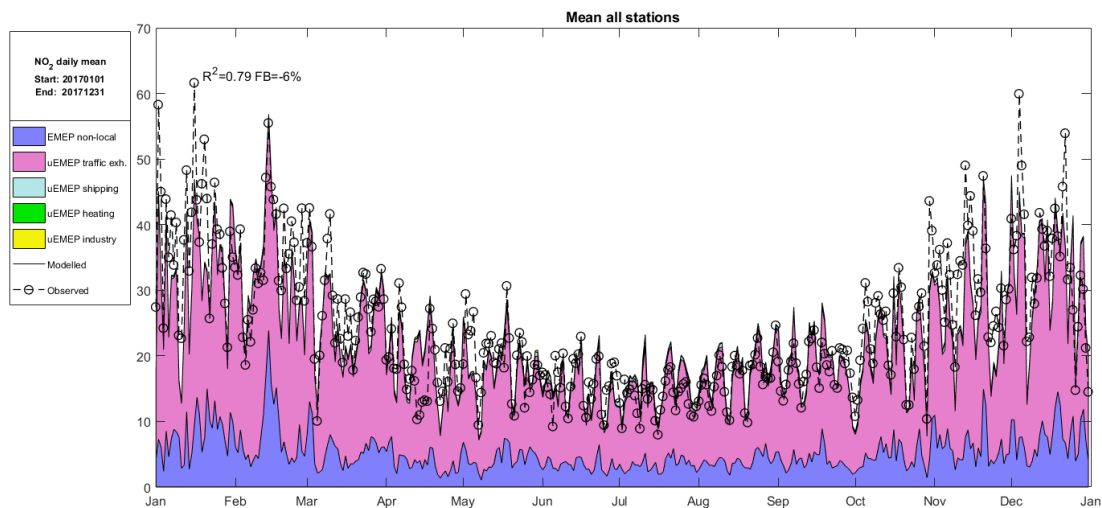
665 **Figure 9. Positions of all 72 monitoring stations in Norway. 33 for PM_{2.5}, 36 for NO₂, 45 for PM₁₀, 8 for O₃**
 (©kartverket/norgeskart.no).

Fig. 10 shows the comparison of modelled and observed NO₂ for annual average at each station (scatter plot) and daily mean temporal profile averaged over all stations. Included in the scatter plot are the Scandinavian EMEP MSC-W results at 2.5 km. The spatial correlation is quite high, $r^2=0.81$ for uEMEP with little negative bias (FB=-5.9%). The temporal variation over the whole year is also well represented when averaged over all stations ($r^2=0.79$).

670



(a)

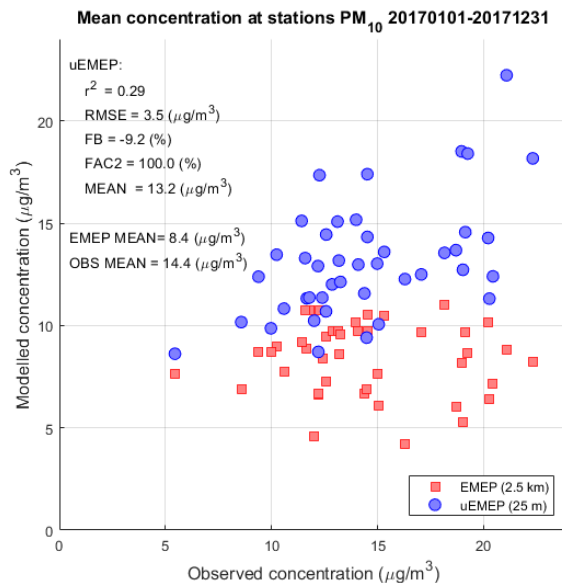


(b)

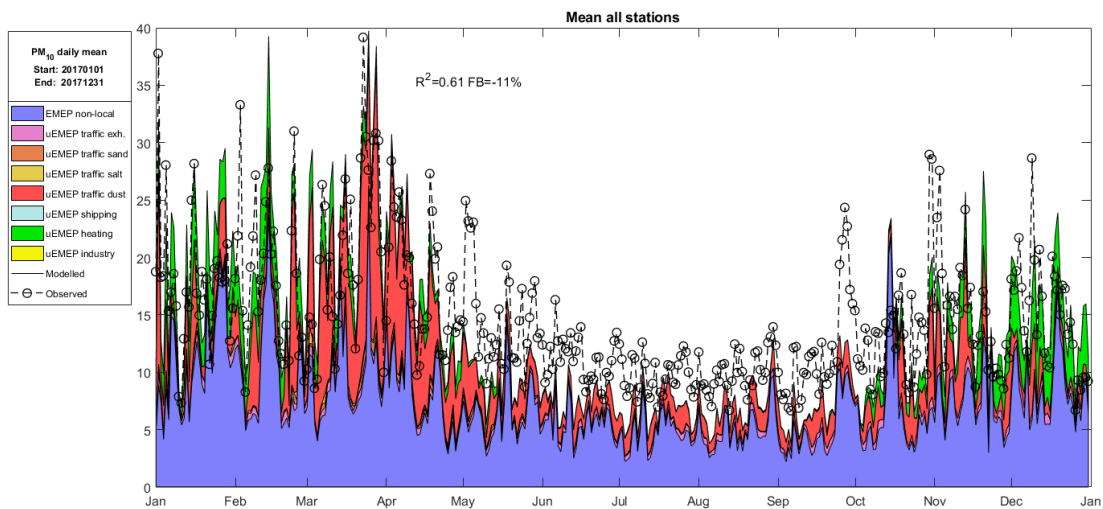
675 **Figure 10. (a) Scatter plot comparison of modelled and observed NO₂ for annual average concentrations at each station. Shown are the results for both uEMEP and EMEP. Comparative statistics are shown for the uEMEP calculation. EMEP and observed means are also included. (b) Daily mean temporal profile averaged over all stations. Source contributions are shown for the temporal modelling results along with the EMEP 2.5 km calculation (EMEP4NO). 36 stations are used in the comparison.**

680 Fig. 11 shows the comparison of modelled and observed PM₁₀ for annual average at each station (scatter plot) and daily mean temporal profile averaged over all stations. Included in the scatter plot are the Scandinavian EMEP results at 2.5 km. The spatial correlation is low, $r^2=0.29$ for uEMEP with little negative bias (FB=-9.2%). The temporal variation over the whole year

is well represented when averaged over all stations ($r^2=0.61$) but the model has a negative bias of $4 \mu\text{g}/\text{m}^3$ over much of the summer period. Road dust events in the spring time are well captured by the emission model NORTRIP.



(a)



(b)

Figure 11. (a) Scatter plot comparison of modelled and observed PM_{10} for annual average concentrations at each station. Shown are the results for both uEMEP and EMEP. Comparative statistics are shown for the uEMEP calculation. EMEP and observed means

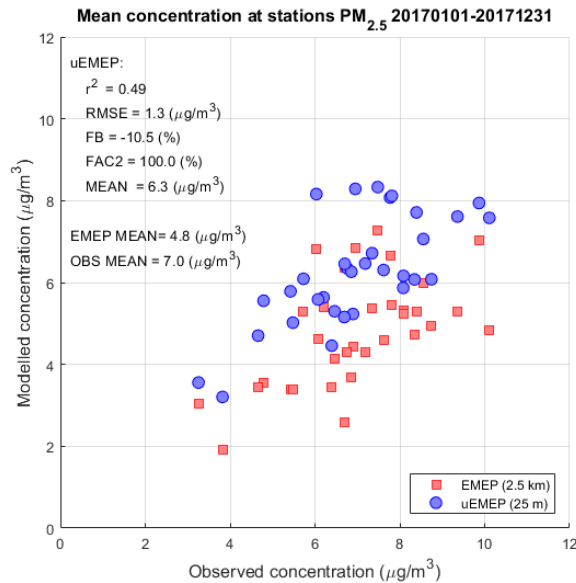
685

690

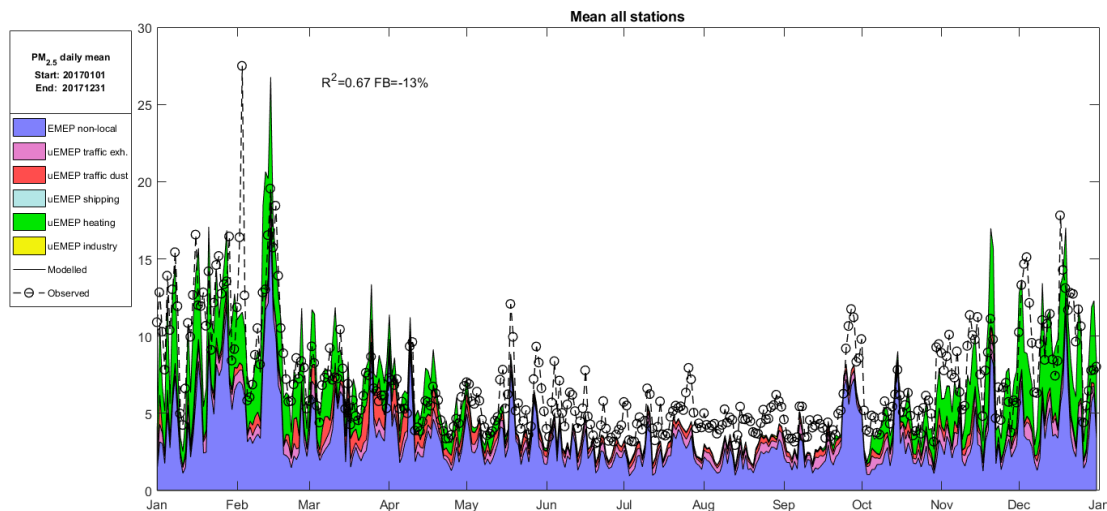
are also included. (b) Source contributions from both uEMEP and EMEP models are shown for the temporal modelling results along with the EMEP 2.5 km calculation (EMEP4NO). 45 stations are used in the comparison.

Fig. 12 shows the comparison of modelled and observed $PM_{2.5}$ for annual average at each station (scatter plot) and daily mean temporal profile averaged over all stations. Included in the scatter plot are the Scandinavian EMEP results at 2.5 km. The spatial correlation is good, $r^2=0.49$ for uEMEP with little negative bias (FB=-10.5%). The temporal variation over the whole year is well represented when averaged over all stations ($r^2=0.67$) but the model has a negative bias of $2 \mu g/m^3$ over much of the summer period. Residential wood combustion (heating) events in the winter are well captured by the emission model MetVed.

700



(a)



(b)

705 **Figure 12. (a) Scatter plot comparison of modelled and observed PM_{2.5} for annual average concentrations at each station. Shown are the results for both uEMEP and EMEP. Comparative statistics are shown for the uEMEP calculation. EMEP and observed means are also included. (b) Source contributions are shown from both uEMEP and EMEP models for the temporal modelling results along with the EMEP 2.5 km calculation (EMEP4NO). 33 stations are used in the comparison.**

5.2 Verification and sensitivity tests

710 In addition to the validation against monitoring data a number of verification and sensitivity experiments have been undertaken with the model. These include:

- Comparison of single annual mean calculations with the mean of hourly calculations
- Sensitivity to the moving window size
- Sensitivity to the choice of resolution
- 715 • Sensitivity to the temperature dependence of NO_x exhaust emissions
- Sensitivity to the choice NO₂/NO_x initial exhaust ratio

These sensitivity tests are provided in the Supplementary material (Sect. S5). We present only conclusions from these.

720 **Comparison of single annual mean calculations with the mean of hourly calculations:**

In Sect. 3 we describe two methods for calculating dispersion. One is based on the hourly meteorological and emission data, Sect. 3.1, and the other on annual mean data, Sect. 3.2. A rotationally symmetric dispersion kernel, Eq. (25), is used for dispersion of the annual mean emissions. Tests using the same dispersion parameters in both annual and hourly calculations, Sect. S5.1, give very similar results for both methodologies indicating the validity of the annual mean calculation. When K_z

725 based dispersion, Eq. (15-23), is used in the hourly calculations then there is a larger difference between the two methods because of the difference between the two dispersion parameterisations. We conclude that the time saving advantage of the single annual mean calculation, approximately 10000 times faster, and the similarity to the hourly calculation make it an efficient and valid method for calculating high resolution annual maps of air quality.

730 **Sensitivity to the moving window size:**

The size of the moving window region within which uEMEP calculates local high resolution concentrations should impact on the results since smaller moving windows will include less locally modelled contributions and more non-local EMEP contributions. This has been verified in a sensitivity study, Supplementary material Sect. S5.2. In this sensitivity experiment the moving window size was varied from $n_{mw} = 1$ to 8 EMEP grids and calculations were made at existing measurement sites.

735 The mean concentrations are shown to be quite insensitive to the choice of this region, particularly for PM₁₀. Generally the reduction in the local contribution is well balanced with the increase in the non-local contribution when reducing the size of the moving window, verifying the methodology. It is recommended to use a minimum of 2 EMEP grids for the moving window region.

740 **Sensitivity to the choice of resolution:**

The choice of sub-grid resolution will impact on the calculated concentrations, both in concentration levels and in spatial distribution. An experiment where a range of sub-grid resolutions were tested, from 15 m to 250 m, was carried out, Sect. S5.3. Calculations were made at the positions of the Norwegian monitoring sites, most of which are traffic sites. The results showed that even at resolutions of 250 m the mean concentrations for all stations were very similar. At 100 m resolution, compared to
745 the reference of 25 m, the difference in annual mean was no larger than 15% at any one station with a normalised root mean square error (NMRSE) of 6%. The NRMSE increased to 11% for the 250 m calculation with a maximum deviation of 40% at one station. We conclude that 100 m resolution will provide good concentration estimates for near road calculations though higher resolutions may be required, depending on the application.

750 **Sensitivity to the temperature dependence of NO_x exhaust emissions:**

The temperature dependence of the NO_x traffic exhaust emissions was assessed by running the model with and without this dependency, Sect. S5.4. With this correction the results show a significant improvement in the station mean time series correlation (from $r^2=0.68$ to 0.79) and improved correlation in both the daily (from $r^2=0.56$ to 0.60) and annual (from $r^2=0.76$ to 0.78) mean calculations. Bias is also reduced from -20% to -3%. The correction factor used, Eq. (S13), still requires further
755 evaluation and should be considered only as an initial estimate.

Sensitivity to the choice NO₂/NO_x initial exhaust ratio:

In the calculations shown in Fig. 10 for NO₂ an initial NO₂/NO_x exhaust emission ratio of 0.25 was used. This reflects the large portion of diesel vehicles used in Norway and the high NO₂/NO_x ratio of these (Hagman, 2011). However, comparison of
760 modelled ratios of NO₂/NO_x indicate this ratio may be too high. This was assessed by running the model with three different ratios, 0.15, 0.25 and 0.35. The results, Sect. S5.5, show that an NO₂/NO_x ratio of 0.15 most closely fits the observed ratio and this ratio will be implemented in further applications of the model.

6. Discussion

The aim of uEMEP is to provide downscaling capabilities for the EMEP MSC-W model with the intention of improving
765 exposure estimates and more realistic concentrations at high resolution over large areas. The example application provided, the Norwegian air quality forecast and expert user service, is an example of how high resolution coverage over large regions (countries) can be achieved. The validation carried out in Sect. 5.1 shows that the modelling system provides moderate to good comparison with observations. The best results are for NO₂, chiefly because we have the best information concerning emissions that contribute to these concentrations, i.e. traffic exhaust. The lower correlation of PM is indicative of the difficulties in
770 modelling emissions such as residential wood burning and road dust emissions. That NO₂ is well modelled indicates that the problems lie largely with the emissions, rather than the dispersion model itself. In addition a large proportion of PM is due to medium to long range transport and secondary formation of particles. This is not part of the uEMEP model but relies on the EMEP MSC-W model and the emissions included there.

775 The strength of the modelling system is in the integration of uEMEP with EMEP through the use of the local fraction. This allows downscaling anywhere within an EMEP domain provided that suitable proxy data is available for the downscaling. This is an important aspect of the modelling and is the link that can bind the regional and local scale emission communities. Usually the proxies used for regional scale emission inventories are not available to the user so that exactly how these emissions are made, quantitatively, is unknown to the user. In addition, as the resolution of regional scale emission inventories increase so
780 too does the need for improved spatial distribution proxies. Population density, successfully used to distribute a range of emission sectors on low resolution grids (> 10 km) is no longer suitable for many sectors since at high resolution the emissions are no longer correlated with population. This was discussed in an earlier paper, Denby et al. 2011, and remains problematic.

When implementing uEMEP it is highly desirable that the emissions used in both uEMEP and EMEP models are consistent
785 with one another. This has been achieved for the Norwegian application for the sectors traffic, domestic heating, shipping and industry. However other sources, such as other mobile combustion sources associated with construction and other activities, are not included. These can be of importance locally even if they are not significant on the regional scale. There is no clear methodology available on how to implement these emissions at the required resolution.

790 The modelling system has limitations. Currently only primary emissions, with the exception of NO₂ formation, are dealt with. Some secondary formation of particles will likely occur within the local region used for the uEMEP model domain but these are not currently accounted for. uEMEP is also a Gaussian model that does not take into account obstacles of any type. When achieving resolutions of 50 m then buildings start to play an important role in the transport and dispersion. The region covered by the local scale modelling, the moving window region, is necessarily limited in extent. Sensitivity studies show that this has
795 limited impact on mean concentrations but for source sectors such as industry, that are released at height, the limited calculation region may not be large enough to include all of the plumes impact region.

In many ways the increase in resolution to almost street level puts new demands on the modelling system that were not necessary to consider previously. For regional scale modellers the downscaling can provide considerable improvement to
800 regional calculations. However, from a local scale modelling perspective, the local scale information may not be of sufficient quality to be useful to local users. This is most important when only proxy data is available for downscaling rather than actual bottom up emissions. In the end, if high resolution modelling is to be used at the local scale then similarly high quality emission data will be required if the results are to be useful to users.

805 There are a number of aspects of the modelling system that can be, and are being, improved. These include:

- Implementation of dry and wet deposition in uEMEP, currently not included in this version
- Improving the annual mean dispersion kernel dispersion parameters to be more consistent with the hourly K_z methodology
- Implementing necessary secondary formation of PM in uEMEP
- 810 • Further assessment of the K_z Gaussian plume methodology
- Refinement of the temperature dependence of NO_x traffic exhaust emissions

A number of aspects were not treated in this paper but will be topics of further studies. These include population exposure and the impact of resolution, trend assessment in emissions and analysis of road dust emissions for all of Norway. In addition, the
815 modelling system is being applied in a number of different countries and results of these applications will be further described and assessed.

7. Conclusion

This paper presents and documents a new downscaling model and method (uEMEP) for use in combination with the EMEP MSC-W chemical transport model. Process descriptions and parameterisations within the uEMEP model are provided and the
820 methodology for combining uEMEP with EMEP MSC-W local fraction calculations is elaborated. An example application, The Norwegian air quality forecast system, is presented and validation for the year 2017 at all available Norwegian air quality

stations is provided. A number of verification and sensitivity studies are summarised in the paper and expanded in the Supplementary material.

825 The uEMEP model provides a new methodology for downscaling regional scale chemical transport models but can currently only be applied together with the EMEP MSC-W model since this is the only model with the necessary local fraction calculation. The uEMEP model is based on Gaussian modelling that has existed for many years but it does use specific parameterisations to describe the dispersion parameters in order to be compatible with the EMEP model application.

830 uEMEP can provide improved exposure estimates if suitable proxy data for emissions are available and can be applied to regions as large as the regional scale CTM in which it is imbedded. It can also represent concentrations down to street level, **though not street canyons**, and is comparable with traffic monitoring sites. This makes it a unique system for assessment, policy application and forecasting purposes.

Code and data availability

835 The current version of uEMEP is available from Github (<https://github.com/metno/uEMEP>) under the licence GNU Lesser General Public License v3.0. The code is written in fortran 90 and is compilable with intel fortran (ifort). The code does not support gfort as a compiler at this time. The exact version of the model used to produce the results used in this paper is archived on Zenodo (DOI: 10.5281/zenodo.3756008), as are input data and scripts to run the model and produce the plots for all the simulations presented in this paper (DOI: 10.5281/zenodo.3755573).

840 **Author contribution**

Bruce Rolstad Denby is the lead author of the article and developer of the uEMEP model. Michael Gauss and Hilde Fagerli internally reviewed and contributed to the writing of the article. Peter Wind is the developer of the local fraction methodology in the EMEP MSC-W model and provided text on this. Qing Mu carried out the EMEP MSC-W calculations for this article and contributed to the text. Eivind Grøtting Wærsted carried out the validation of the uEMEP model and contributed to the
845 text. Alvaro Valdebenito and Heiko Klein provided the technical support for carrying out the modelling and contributed to the uEMEP code and associated scripts for its implementation.

Acknowledgements

uEMEP was developed and applied with financing from the Research Council of Norway (NFR) project 'AirQuip' (grant no. 267734), The Norwegian Public Roads Administration (Statens Vegvesen), the Norwegian Environment Agency (Miljødirektoratet) and the Ministry of Climate and Environment (Klima- og miljødepartementet).

References

- Andersson, C., Langner, J., and Bergström, R.: Interannual variation and trends in air pollution over Europe due to climate variability during 1958–2001 simulated with a regional CTM coupled to the ERA40 reanalysis, *Tellus*, 59B, 77–98, doi:10.1111/j.1600-0889.2006.00196.x, 2007.
- Appel, K. W., Napelenok, S. L., Foley, K. M., Pye, H. O. T., Hogrefe, C., Luecken, D. J., Bash, J. O., Roselle, S. J., Pleim, J. E., Foroutan, H., Hutzell, W. T., Pouliot, G. A., Sarwar, G., Fahey, K. M., Gantt, B., Gilliam, R. C., Heath, N. K., Kang, D., Mathur, R., Schwede, D. B., Spero, T. L., Wong, D. C., and Young, J. O.: Description and evaluation of the Community Multiscale Air Quality (CMAQ) modeling system version 5.1, *Geosci. Model Dev.*, 10, 1703–1732, doi:10.5194/gmd-10-1703-2017, 2017.
- Bächlin, W., Bösinger, R.: Untersuchungen zu Stickstoffdioxid-Konzentrationen, Los 1 Überprüfung der Rombergformel. Ingenieurbüro Lohmeyer GmbH & Co. KG, Karlsruhe. Projekt 60976-04-01, Stand: Dezember 2008. Gutachten im Auftrag von: Landesamt für Natur, Umwelt und Verbraucherschutz Nordrhein--Westfalen, Recklinghausen, 2008.
- Benson, P.: A review of the development and application of the CALINE3 and 4 models. *Atmos. Environ.* 26B:3, 379-390, doi:10.1016/0957-1272(92)90013-I, 1992.
- Benson, P.: CALINE4 – A dispersion model for predicting air pollutant concentrations near roadways. FHWA/CA/TL-84/15, California Department of Transportation, Sacramento, CA, 1984. URL: <https://ntrl.ntis.gov/NTRL/dashboard/searchResults.xhtml?searchQuery=PB85211498>
- Brandt, J., Christensen, J., Frohn, L. and Zlatev, Z.: Operational air pollution forecast modelling using the THOR system. *Physics and Chemistry of the Earth, Part B: Hydrology, Oceans and Atmosphere*, 26, 117-122, doi:10.1016/S1464-1909(00)00227-6., 2001.

- CAMS: Copernicus Atmosphere Modelling Service (CAMS), Air quality forecasts Europe, 2020. URL: <https://atmosphere.copernicus.eu/>
- 880
- Chaudhry, F.H., Meroney, R.H.: Similarity theory of diffusion and the observed vertical spread in the diabatic surface layer. *Boundary-Layer Meteorol.* 3, 405-415, doi:10.1007/BF01034984, 1973
- Cimorelli, A.J., Perry, S.G., Venkatram, A., Weil, J.C., Pain, R.J., Wilson, R.B., Lee, R.F., Peters, W.D., Brode, R.W.,
885 Paumier, J.O.: AERMOD: Description of model formulation, EPA-454/R-03-004. doi:EPA-454/R-03-004, 2004.
- Denby, B., Cassiani, M., de Smet, P., de Leeuw, F. and Horálek, J.: Sub-grid variability and its impact on European wide air quality exposure assessment, *Atmos. Environ.*, 45, 4220-4229, doi:10.1016/j.atmosenv.2011.05.007, 2011
- 890 Denby, B.R.: Guide on modelling Nitrogen Dioxide (NO₂) for air quality assessment and planning relevant to the European Air Quality Directive. ETC/ACM Technical paper 2011/15, 2011. URL: https://www.eionet.europa.eu/etcs/etc-atni/products/etc-atni-reports/etcacm_tp_2011_15_fairmode_guide_modelling_no2
- ECMWF, 2020. URL: www.ecmwf.int
- 895
- Garratt, J.R.: *The Atmospheric Boundary Layer*, Cambridge Univ. Press, Cambridge, U.K., 316 pp, 1994.
- Golder, D.: Relations among stability parameters in the surface layer, *Boundary-Layer Meteorol.*, 3, 47–58, doi:10.1007/BF00769106, 1972.
- 900
- Granier, C., S. Darras, H. Denier van der Gon, J. Doubalova, N. Elguindi, B. Galle, M. Gauss, M. Guevara, J.-P. Jalkanen, J. Kuenen, C. Liousse, B. Quack, D. Simpson and K. Sindelarova: The Copernicus Atmosphere Monitoring Service global and regional emissions (April 2019 version), Report April 2019 version, null, doi:10.24380/d0bn-kx16, 2019
- 905 Green A.E.S., Singhal R.P. and Venkateswar R.: Analytic extensions of the gaussian plume model, *Journal of the Air Pollution Control Association*, 30(7) , 773-776, doi:10.1080/00022470.1980.10465108, 1980.
- Gryning, S., Batchvarova, E. and Brümmner, B.: On the extension of the wind profile over homogeneous terrain beyond the surface boundary layer, *Boundary-Layer Meteorol.*, 124, 251–268, doi:10.1007/s10546-007-9166-9, 2007.
- 910

- Hagman, R., Gjerstad, K.I. & Amundsen, A.H., 2011. NO₂-utslipp fra kjøretøyparken i norske storbyer, TØI rapport 1168/2011: Transportøkonomisk institutt, Oslo. <https://www.toi.no/getfile.php?mmfileid=22618>
- 915 Hanna SR (1981) Lagrangian and Eulerian time-scale in the daytime boundary layer. *J Appl Meteorol* 20:242–249
- IFS: Documentation of the Integrated Forecasting System, ECMWF, 2020. URL: <https://www.ecmwf.int/en/publications/ifs-documentation>
- 920 Karamchandani, P., Lohman, K. & Seigneur, C.: Using a sub-grid scale modeling approach to simulate the transport and fate of toxic air pollutants. *Environ. Fluid Mech.* 9, 59–71, doi:10.1007/s10652-008-9097-0, 2009.
- Karl, M., Walker, S.-E., Solberg, S., and Ramacher, M. O. P.: The Eulerian urban dispersion model EPISODE – Part 2: Extensions to the source dispersion and photochemistry for EPISODE–CityChem v1.2 and its application to the city of Hamburg, *Geosci. Model Dev.*, 12, 3357–3399, doi:10.5194/gmd-12-3357-2019, 2019.
- 925 Kim, Y., Wu, Y., Seigneur, C., and Roustan, Y.: Multi-scale modeling of urban air pollution: development and application of a Street-in-Grid model (v1.0) by coupling MUNICH (v1.0) and Polair3D (v1.8.1), *Geosci. Model Dev.*, 11, 611–629, doi:10.5194/gmd-11-611-2018, 2018.
- 930 Kranenburg, R., Segers, A. J., Hendriks, C., and Schaap, M.: Source apportionment using LOTOS-EUROS: module description and evaluation, *Geosci. Model Dev.*, 6, 721–733, doi:10.5194/gmd-6-721-2013, 2013.
- 935 Kuenen, J. J. P., Visschedijk, A. J. H., Jozwicka, M., and Denier van der Gon, H. A. C.: TNO-MACC_II emission inventory; a multi-year (2003–2009) consistent high-resolution European emission inventory for air quality modelling, *Atmos. Chem. Phys.*, 14, 10963–10976, 2014 doi:10.5194/acp-14-10963-2014
- Liu, X., Godbole, A., Lu, C., Michal, G. and Venton, P.: Optimisation of dispersion parameters of Gaussian plume model for CO₂ dispersion. *Environmental science and pollution research international*, 22, doi:10.1007/s11356-015-5404-8, 2015.
- 940 Maiheu, B., Williams, M. L., Walton, H. A., Janssen, S., Blyth, L., Velderman, N., Lefebvre, W., Vanhulzel, M. and Beevers, S. D. Improved Methodologies for NO₂ Exposure Assessment in the EU, Vito Report no.: 2017/RMA/R/1250, 2017. URL: <http://ec.europa.eu/environment/air/publications/models.htm>

- Martin, D.O.: Comment on “The Change of Concentration Standard Deviations with Distance”, Journal of the Air Pollution Control Association, 26, 145-147, doi:10.1080/00022470.1976.10470238, 1976.
945
- Menut, L., Bessagnet, B., Khvorostyanov, D., Beekmann, M., Blond, N., Colette, A., Coll, I., Curci, G., Foret, G., Hodzic, A., Mailler, S., Meleux, F., Monge, J.-L., Pison, I., Siour, G., Turquety, S., Valari, M., Vautard, R., Vivanco, M.G.: CHIMERE 2013: a model for regional atmospheric composition modelling. Geosci. Model Dev., 6, 981–1028. doi:10.5194/gmd-6-981-
950 2013, 2013.
- Müller, M., M. Homleid, K. Ivarsson, M.A. Køltzow, M. Lindskog, K.H. Midtbø, U. Andrae, T. Aspeli, L. Berggren, D. Bjørge, P. Dahlgren, J. Kristiansen, R. Randriamampianina, M. Ridal, and O. Vignes: AROME-MetCoOp: A Nordic Convective-Scale Operational Weather Prediction Model. Wea. Forecasting, 32, 609–627, doi:10.1175/WAF-D-16-0099.1,
955 2017
- Nieuwstadt, F.T.M.: Some aspects of the turbulent stable boundary layer. Boundary-Layer Meteorol., 30, 31–55, doi:10.1007/BF00121948, 1984.
- 960 Norwegian air quality forecasting service, 2020. URL: <https://luftkvalitet.miljostatus.no/>
- Norwegian air quality expert user service, 2020. URL: <https://www.miljodirektoratet.no/tjenester/fagbrukertjeneste-for-luftkvalitet/>
- 965 Romberg E., Böisinger, R., Lohmeyer, A., Ruhnke, R., Röth, R.: NO-NO₂-Umwandlung für die Anwendung bei Immissionsprognosen für Kfz-Abgase. In: Staub-Reinhaltung der Luft, 56 (6), 215-218, 1996. URL: <https://publikationen.bibliothek.kit.edu/1000065362>
- Sauter, F., van Zanten, M., van der Swaluw, E., Aben, J., de Leeuw, F., van Jaarsveld, H.: The OPS-model. Description of
970 OPS 4.5.2., 2018. URL: <https://www.rivm.nl/media/ops/v4.5.2/OPS-model-v4.5.2.pdf>
- Seinfeld, J. H. and Pandis, S. N. (1998). Atmospheric Chemistry and Physics from air pollution to climate change. New York. John Wiley and Sons, Incorporated.
- 975 Simpson, D., Benedictow, A., Berge, H., Bergström, R., Emberson, L. D., Fagerli, H., Flechard, C. R., Hayman, G. D., Gauss, M., Jonson, J. E., Jenkin, M. E., Nyiri, A., Richter, C., Semeena, V. S., Tsyro, S., Tuovinen, J.-P., Valdebenito, Á., and Wind,

- P.: The EMEP MSC-W chemical transport model – technical description, *Atmos. Chem. Phys.*, 12, 7825–7865, doi:10.5194/acp-12-7825-2012, 2012.
- 980 Smith M.E. (ed) (1973). Recommended Guide for the Prediction of the Dispersion of Airborne Effluents. Vol. 2 Amer. Soc.Mech. Eng., New York, 85 pp.
- Sofiev, M., Vira, J., Kouznetsov, R., Prank, M., Soares, J., and Genikhovich, E.: Construction of the SILAM Eulerian atmospheric dispersion model based on the advection algorithm of Michael Galperin, *Geosci. Model Dev.*, 8, 3497–3522, 985 doi:10.5194/gmd-8-3497-2015, 2015.
- Stocker, J., Hood, C., Carruthers, D., McHugh, C.: ADMS-Urban: developments in modelling dispersion from the city scale to the local scale, *Int. J. Environ. Pollut.* 50, 308. doi:10.1504/IJEP.2012.051202, 2012
- 990 Tarrason, L., Hamer, P., Meleux, F., and Rouil, L.: Interim Annual Assessment Report. European air quality in 2017, Tech. Rep. CAMS71_2018SC3_D71.1.1.10_IAAR2017_final, 2018. URL: https://policy.atmosphere.copernicus.eu/reports/CAMS71_D71.1.1.10_201807_IAAR2017_final.pdf
- Theobald, M. R., Simpson, D., and Vieno, M.: Improving the spatial resolution of air-quality modelling at a European scale – 995 development and evaluation of the Air Quality Re-gridder Model (AQR v1.1), *Geosci. Model Dev.*, 9, 4475–4489, doi:10.5194/gmd-9-4475-2016, 2016.
- Turner, D. B.: Workbook of Atmospheric Dispersion Estimates: An Introduction to Dispersion Modeling, Second Edition 2nd Edition. CRC Press Published May 5, 1994, 192 Pages, ISBN 9781566700238 - CAT# L1023 1000
- van Ulden, A.P.: Simple estimates from vertical dispersion from sources near the ground, *Atmos. Environ.* 12, 2125-2129, doi:10.1016/0004-6981(78)90167-1, 1978.
- Venkatram, A., Strimaitis, D. and Dicristofaro, D.: A semiempirical model to estimate vertical dispersion of elevated releases 1005 in the stable boundary layer, *Atmos. Environ.*, 18(5), 923-928, doi:10.1016/0004-6981(84)90068-4, 1984.
- Venkatram, A: An examination of the Pasquill-Gifford-Turner dispersion scheme, *Atmos. Environ.*, 30(8), 1283-1290, doi:10.1016/1352-2310(95)00367-3, 1996.

1010 Venkatram, A., Snyder, M.G., Heist, D.K., Perry, S.G., Petersen, W.B. and Isakov, V.: Re-formulation of plume spread for near-surface dispersion, *Atmos. Environ.*, 77, 2013, 846-855, doi:10.1016/j.atmosenv.2013.05.073, 2013.

Vizcaino, P. and Lavallo, C.: Development of European NO₂ Land Use Regression Model for present and future exposure assessment: Implications for policy analysis, *Environmental Pollution*, 240, 140-154, doi:10.1016/j.envpol.2018.03.075, 2018.

1015

Werner, M., Kryza, M. and Wind, P.: High resolution application of the EMEP MSC-W model over Eastern Europe – Analysis of the EMEP4PL results, *Atmospheric Research*, 212, 6-22, doi:10.1016/j.atmosres.2018.04.025, 2018.

1020 Wind, P., Rolstad Denby, B., and Gauss, M.: Local fractions – a method for the calculation of local source contributions to air pollution, illustrated by examples using the EMEP MSC-W model (rv4_33), *Geosci. Model Dev.*, 13, 1623–1634, <https://doi.org/10.5194/gmd-13-1623-2020>, 2020.

1025 REVIEWER 1

Thanks to reviewer 1 for their very detailed review. The manuscript has definitely been improved because of these comments.
Here follows the authors answers/comments to the review

1030

- Line 46: the Authors could mention the OSPM model as an example of a streetcanyon model to complement the overview of local scale models

* The two examples given are of urban modelling systems. OSPM is a street canyon model, not a system for modelling whole urban regions. It is part of the THOR forecast system as the last part of the cascade. We did not include it in this line but it is implicitly include via the THOR reference.

1035

- Line 95: clarify if this option implies that emissions in the EMEP grid cell are not consistent with the ones in the sub-grid cells

1040

* This is clarified with the text. 'The independent emissions do not need to be consistent with the EMEP gridded emissions in this case.'

- Line 101: some discussion on the implications of using such inconsistent chemistry treatments in uEMEP and EMEP would be appreciated. As uEMEP is intended for applications over wide regions with significantly different chemical regimes, the simple chemistry may perform better in some environments than others

1045

* This we have commented in Section 3.4 and 3.5 where this is discussed. In Section 3.4 we have added 'Comparisons with EMEP NO₂ calculations show that this chemistry scheme matches the results obtained by EMEP over longer time periods.' and in Section 3.5 with 'This empirical relationship will vary from region to region, largely due to differences in O₃ concentrations and photolysis rates that are not included as part of the parameterization. If used over large regions, for example Europe, then the uncertainty in the NO₂ conversion will increase.'

1050

- Line 116 and 140: the term $C_{sg_nonlocal}(i,j)$ is the more complex to understand. Perhaps, an equation describing how is computed would help the reader. I appreciate the effort of the Authors to explain the method with Figure 1 and 2 and Section 2.3,

1055

but it is still confusing how the local and non-local contributions of the EMEP grids are used in the computation of the Csg_nonlocal term.

1060

* We are aware that the non-local, local and the moving window concepts may not be as clear as we would like but we have tried to explain this as best we can. These are geometrical considerations that are not easy to express in words or even equations and best explained on whiteboards or with pen and paper. However, the reviewer has pointed out an oversight in our text. In actual fact Csg_nonlocal (Equation 1) is equivalent to Cg_nonlocal derived in Equation 10, since it is the EMEP contribution to the non-local subgrid. This was not explicitly mentioned but Equation 10 has now been updated, along with the text, to indicate this.

1065

- Line 147: More details on Wind et al. (2020) methodology would be appreciated in the manuscript. Considering that the local fraction estimate links emissions with concentrations, the Authors could clarify how the chemistry is treated once the tagged emissions are dispersed in the EMEP grid cells. Are tagged primary pollutants emitted as inert tracers or limited chemistry is considered? The details are provided in Wind et al. (2020), but the reader would appreciate some further descriptions of the method and limitations in the present manuscript.

1070

1075

* We have included the following sentence concerning chemistry 'Tagged species are assumed to be inert species, primary PM and NOX, for the downscaling application as chemical reactions are not included in the tagging.'

- Line 152: Provide which fraction of the total contribution is missed in the local fraction estimate when using few EMEP grid cells.

1080

* The authors perhaps did not understand how to answer this question. If all EMEP grids for the local fraction, not just 5 x 5, were used then 100% would be included. With less grids more will be part of the EMEP non-local contribution and less a part of the uEMEP local calculation. We attempt to address this in the sensitivity tests given in Sections 5.2 and S5.2. There we show for example that when increasing the moving window size from 4 to 8 EMEP grids then the local contribution increases by just 4% for PM10 and for NO2 this is 7%. There is no single answer to the reviewer's question so none can be given in the text. The reader is already referred to this sensitivity study in the text.

1085

- Line 178 Eq. 6: Why this is not divided by the sum of the weights? Following the example in Fig. 1, you use more than 9 EMEP grid cells (adding their concentration) to obtain the local contribution of the moving window over the i,j sub-grid cell. This results

1090

with a local contribution overestimated somehow if $nmw > 1$. For the case $nmw = 1$, the expression seems good as the sum of the weights would be 1.

1095 * The local fraction calculation from EMEP specifies in the 5 x 5 grids surrounding each grid how much that grid contributes to the central grid (Cg_local). So if all the weights (w) were 1 we would simply get the sum of all the contributions to that central grid within that area. The weighting is just to account for when a part of the grid is included in the moving window. Having read the reviewers question we see there may be some confusion concerning the notation. The terms $Cg_local(I,J)$ refers to the contribution to any one EMEP grid from the surrounding grids. We left off this index to avoid over indexing, 1100 though this indexing is included in the Wind article. We will put this additional indexing back into the $Cg_local(I,J,I_lf,J_lf)$ where I,J refer to the grid and I_lf, J_lf refer to the local fraction grid associated with each I,J grid and where I_lf and J_lf are indexed from $-n_lf/2:n_lf/2$. We thank the reviewer for this comment that, though indirectly, corrected a misunderstanding in the notation.

1105 - Line 233 Eq. 10: Why $Cg(i,j,s)$ is divided by $nsource$ if it is already the concentration of a specific source?

* In Eq. 10 $Cg(i,j,s)$ is the sum of the moving window total concentrations calculated for each source, i.e. $Cg(i,j,s) = Cg_local(i,j,s) + Cg_nonlocal(i,j,s)$. This was not specified in the paper so Equation 10 has been rewritten to reflect 1110 this. As written in the text the non-local and local contributions can be different for each source when using the emissions for weighting and each source will have a nonlocal component contributed from the other sources. So after doing this source specific calculation these must be recombined into a single nonlocal concentration. This is done in Equation 10 by taking the average of all the source specific total concentration calculations $Cg(i,j,s)$ and then subtracting the total local contribution to get the final non-local value. This is rigorously correct when using the area weighting but is only a very close estimate when 1115 using the emission weighting. The authors realise that including the emission weighting makes this section much more complicated than otherwise required if only area weighting was used. To clarify what is being done the paragraph before Eq. 10 has been altered to read "These local and non-local calculations are carried out for each emission source individually so the non-local contribution is also dependent on source and the non-local component for any particular source will also contain the local contributions from the other sources. This makes creating a final non-local contribution complicated. To solve this all 1120 the source specific $Cg_local + Cg_nonlocal$ contributions are averaged and the sum of the Cg_local source contributions are subtracted to obtain the final $Cg_nonlocal$. The final non-local contribution at each sub-grid $Csg_nonlocal$, Eq.(1), is equivalent to the EMEP non-local $Cg_nonlocal$ contribution and is calculated by '

1125 - Line 295: I suggest introducing in this section the meandering and traffic term described in the supplementary material. Some variables in the equations are not defined just before or after presenting the equation. It would help the reader to introduce

all the terms after the equations and specify which ones will be further described in subsequent sections

1130 * We have included the following paragraph in this Section 'In addition to the parameterizations presented here uEMEP also includes parameterizations, provided in the supplementary material, for plume meandering and change of wind direction (Sec. S3.4.1), traffic induced initial dispersion (Sec. S3.4.3) and road tunnel internal deposition and emissions (Sec. S3.4.5).' and have defined all variables included in these equations.

1135 - Line 330: Mention the floor value of the wind speed imposed in the model in this part of the manuscript. Some details are only presented in the supplementary material.

* The following sentence has been added 'A minimum wind speed of 0.5 m/s for all dispersion calculations has been imposed.'

1140 - Line 414: a table with the sigma_init_y values per emission source would be appreciated.

* The sigma_init_y, as mentioned in the text, is defined almost exclusively by the grid size, rather than the physical process but we have included the additional text 'traffic and 5 m for shipping, heating and industry'

1145 - Line 518: an order of magnitude of the maximum distance allowed in the dispersion of the Gaussian model would be appreciated (i.e., 250 m).

1150 * It is not clear to the authors what the reviewer is referring to here as there is no mention of this in this line. We do not know which 'maximum distance allowed' the reviewer is referring to. The distance the plume can travel is defined by the size of the moving window, if that was what is meant here. If the reviewer is referring to the sub-grid size then there is no numerical limit but we have never applied the model to a larger sub-grid than 500 m.

- Line 583: Is ozone also a product used from uEMEP? Is there any evaluation done for this pollutant?

1155 * Ozone is a product and this is also assessed but we simply did not include it here. There are very few ozone stations in Norway where the model was assessed. This link shows extensive evaluation, also for ozone, but is in Norwegian (<https://www.met.no/prosjekter/luftkvalitet/evaluering-av-luftkvalitets-modellen>)

- Line 631: Some discussion about the improvement in the daily cycle of the uEMEP

1160 results compared with EMEP would be appreciated. Local models use to improve the
traffic peaks but also may inherit issues with the temporal profiles and the boundary
layer evolution. The validation section could be improved introducing some discrimination between types of sites (rural,
industrial, suburban, urban). I suggest presenting all
the material of subsections 5.1.1, 5.1.2 and 5.1.3 under section 5.1 as those sections
1165 consist only in a single paragraph.

* We have reduced Section 5.1 to a single section, as suggested by the reviewer. As listed there are a limited number of
monitoring sites in Norway, with 90% being traffic stations. There is 1 urban site, 3 suburban sites, 2 rural sites and 1 industrial
site. This lack of representation does not warrant individual selection and presentation. The EMEP model run in Norway uses
1170 the same emission data as the local scale uEMEP, only aggregated to grids. So the traffic variation is exactly the same, if this
is what the reviewer is referring to. In general we have tried to keep the validation to a minimum as this will be more thoroughly
assessed at a later date. The validation is intended to show that the model works, rather than a detailed analysis. The paper is
intended as a model description primarily.

1175 - Line 653: What missing processes could explain the remaining bias during the summer period in both PM10 and PM2.5?

* We believe a large part is secondary organics, but that is currently just speculation so this was not taken up in the article. We
intend a more detailed evaluation of many more years in a later article.

1180 - Line 700: it is counter-intuitive having more non-local EMEP contributions with smaller
moving windows. Could the Authors clarify this in the text? If less EMEP grid cells are
used in the moving window, less non-local contributions would be expected.

* Non-local contributions come from outside the moving window. The larger the moving window the less comes from outside
1185 so this is intuitively correct. Said differently, the larger the moving window the more local contribution as well. This is described
in Section S5.2.

- Line 796: There are still some street-canyon processes that uEMEP cannot represent,
particularly in compact cities with high street aspect ratios. The Authors should mention
1190 this in this last concluding remark.

* We have added the text to this line 'It can also represent concentrations down to street level, though not street canyons, '. It
was pointed out before that it is not obstacle resolving but it does not hurt to mention this a second time.

1195 - Line 29: the acronym CTM is used several times in the manuscript but defined in Line 71. Please, define the acronym already in the introduction and use directly the acronym in the rest of the manuscript.

* Done

1200

- Line 51: use coma instead of a semi-colon in the reference

* Done

1205 - Line 58: the reference Wind et al. (2020) is not provided in the reference section.

* That was strange, but inserted.

1210 - Line 154: fix the Section number. Here and in other parts of the manuscript, the number of the reference to specific sections is 0.

* Due to automatic reference system that stopped working. This is now fixed

1215 - Line 245: Use Eq. instead of Equ. in the Figure caption.

* Done

- Line 362: Monin–Obukhov is mistyped in different parts of the manuscript.

1220 * Done

- Line 362: the Monin-Obukhov length and the surface roughness have already been used before in the manuscript. Define them there only once.

1225 * Done

- Line 371 Table1: please, use consistent notation for the boundary layer height and

Monin-Obukhov length. Both have been introduced before as H and L

1230 * Done

- Line 407 and 574: fix the section number that appears in the reference Sect. 0.

* Done

1235

- Line 646: the statistics presented in panel (a) should be introduced in the caption specifying for which model are computed. In panel (b), the Authors could remove the shipping and industry labels in the legend as no information is shown in the figure.

1240 * The contribution from industry and shipping is present but very small, in this case. Since these were calculated we will keep them in the legend. We have added in the figure caption that the statistics in panel (a) refer to the uEMEP model and we have reorganised the statistics text in the plot itself to better reflect this.

1245 - Line 661: There is too much information in Figure 11. I suggest presenting the nonlocal contribution of EMEP and not the detailed composition of it. Though of interest, it is impossible to appreciate EMEP4NO line and some artefacts appear as the white contribution above EMEP PRIMARY blue fraction.

1250 * We agree that the plot was very busy and we have now aggregated all species into the non-local EMEP, as suggested by the reviewer.

- Line 679: avoid using subsections that consist of a single paragraph.

1255 * The authors used this form to have consistent cross referencing to the supplementary material but understand it would seem a little strange in this context. We have removed the numbering but have kept the headings to delineate between the different sensitivity studies.

1260 - Line 719: to be consistent with the supplementary material the coefficient of determination of the station mean time series of uEMEP should be 0.79, not 0.80. Harmonise the number in both documents

* Done

- Line 728: I suggest merging Sections 6 and 7.

1265

* The authors would like to keep these as two separate sections, as is often the case for discussion and conclusion.

- Line 13: Use section S1 instead of S3 and number accordingly the rest

1270

* As explained in the text we use this numbering so it is easy to cross reference between supplementary material and the main document. Given the nature of the supplementary material, that it provides extra details on particular sections in the main document, the authors feel this method of numbering is more appropriate and will keep it. This is already stated at the start of the document.

1275

- Line 106: It should be Eq. (15a).

* Done

- Line 242: Why the inverse of the wind speed is used instead of wind speed?

1280

* In dispersion calculations it is the inverse wind speed that is multiplied with emissions and the dispersion intensity to determine the concentration, Eq. 11. When averaging then it is the mean of the inverse of the wind speed that should be used, rather than the mean of the wind speed.

1285

- Line 314: In the figure caption, it should be Fig. S4 instead of S2.

* Done

- Line 328: The observation measurement could be provided in Fig. S6.

1290

* The comparison with observations has already been made in Figure 10a in the main paper. Since the major aim of this sensitivity study was to assess the dependence on resolution the authors do not think it is necessary to repeat that comparison here, in an already crowded plot. We do not include the observations again here.

1295

- Line 368: Why Figure S8a is different from Figure 10b? The caption describes the

same results.

1300 * The reviewers are correct that these two plots should be the same. This has now been fixed. The discrepancy was due to the way concurrent measurements and model results were selected. The reviewers will also note that the mean of scatter plots is not always the same as the mean of the time series. This is also due to the selection criteria for annual means requiring 75% coverage per station whilst daily mean plots of the average of all stations do not have the same requirement.

- Line 385: A value of 0.1 would likely provide an even closer fit to observations.

1305 * A lower value than 0.15 would probably give a better fit but this was not assessed as it lay outside the expected NO₂/NO_x emission ratio range for vehicles in Norway.

1310 REVIEWER 2

1315 Thanks to reviewer 2 for their comments and time. Some aspects of the modelling, particularly how the local window local/non-local works are difficult to explain but I have tried to improve on this. Reviewer 1 also commented on this. Here follows the answers to the reviewers questions and improvements.

- line 33 / “near street level modelling”: What is then the ambition of the model? Is it supposed to represent concentrations at roadside monitoring sites or background sites?

1320 * It will represent concentrations at roadside monitoring sites, and the validation for NO₂ confirms this, when using a resolution of 25 m. Even so the sensitivity tests to resolution, Section S5.3, show that good results are still obtained at 100 m. It does not however well represent street canyon sites as the Gaussian model used has no obstacles. One would then expect an underestimate at these sites.

1325 - What is the meaning of resolution <100m when there is no local topography modelling involved? Wouldn't building layout, air flows in the street canyon etc need to be accounted for at these very local scales?

1330 * Without including obstacles the increased resolution allows the concentration gradients at roadside to be better described. The reviewer is right to point out that, if this was to be done properly at < 100 m, then buildings need to be included. However, uEMEP is intended for application over country scales and that level of detail is not achievable.

- line 85: Which source sectors are included in the uEMEP downscaling calculations?

1335 Traffic, residential, any other? Should be mentioned somewhere in Sect 2.1

* The downscaled sectors depend on the application so this is not explicitly named until the application is defined in Section 4.2. However, we have included the following text in Section 2.1, line 100 'Typical source sectors downscaled using uEMEP include traffic, residential combustion, shipping and industry. The sectors addressed will depend on the availability of high resolution data for distributing them'

1340

- line 150. "neighbour cells" sounds as if only +/- 1 in each direction but I understand from the next sentence that the local fraction region can be quite large. Please clarify in the text.

1345

* We have changed that sentence to read 'The local fraction region extent is then limited.'

- line 153. Perhaps I missed it but it would be good to have a paragraph somewhere that explains the difference between the different domains (uEMEP vs local fraction vs moving window) as it is a bit confusing to the reader

1350

* Moving window and EMEP local fraction region are described in the text separately but these are also visualised in Fig. 1. That was indeed the intention of Fig. 1. We believe this is sufficient explanation.

1355 - Sect 2.3-2.4: These sections are difficult to follow, I would suggest restructuring 2.3 and 2.4 into one (The second sentence of 2.3 already refers to 2.4)

* We would prefer to keep these as two different sections. The first (2.3) applies to the local fraction calculation from EMEP and the second (2.4) the moving window calculation in uEMEP. Though the second utilises the first, they are two distinct calculations. Reviewer 1 also commented on this section and as a result additional text and a change in formulation of the equations have been implemented. We believe this has helped to clarify these sections.

1360

- Sect 2.4: This is rather complicated to follow for an effect that is probably second order. How much is gained by the complicated moving window calculation of nonlocal contributions at sub-grid resolution? With a reasonably big local fraction tracking domain, the difference between sub-grid and grid level non-local contribution should become negligible?

* The reviewer is correct, first that it is complicated and second that it would not matter if the local fraction domain and moving window were sufficiently large. This is also stated in the text. However, there will always be an edge somewhere to the moving window domain and we consider it necessary to implement a method that can deal with this limit properly, especially when just 1 large EMEP grid, for example 15 km, is used.

- Line 214-216 are a bit confusing, please explain better why this method (as opposed to the area weighting) gives different total (local?) concentrations

* We have tried to clarify this in the text with an extended explanation 'The resulting total concentration, using this method, may be higher or lower than the original EMEP concentrations because it reflects the impact of moving the EMEP grid in space. This is easiest to visualise if the moving window is the same size as the EMEP grid. If the moving window were centred on an area with concentrated emissions, that are in reality spread over two EMEP grids, then when using the emission weighting the new EMEP local contribution would be higher, the non-local lower and the total would be different, see Fig. 2. The opposite is also true if the moving window were placed over a region with low emissions, the local contribution would be lower and the non-local higher. Due to this, it is not possible simply to subtract the local EMEP contribution from the total to get the non-local EMEP contribution, as detailed in Eq. 5.'

- line 218: non-local contributions do not have any associated emission: that is considered in the uEMEP. In general I assume they do have an associated emission. Do s refer to all source sectors in the EMEP model or only those considered in uEMEP?

* We are referring only to the sources that are downscaled using uEMEP but we have reworded to make this clear. 'The first term is the non-local contribution for a particular source and is calculated with the area weighting distribution since non-local contributions, those outside the local fraction region, do not have any associated emission or local fraction for weighting.'

- line 220/ Eq 9 is confusing to me. It should be possible to slightly rephrase the paragraph before to clarify why this needs to be done and what is done here. Also, is there an inconsistency between Eq 6 and Eq 9 regarding the source grid range, Eq 6

has $I-nmw/2 \dots I+nmw/2$ but here it runs from $I-nmw \dots I+nmw$

* The reviewer is correct, there is an inconsistency between Eq. 6 and 9. Thank you pointing this out. We have corrected Eq. 9. Reviewer 1 also commented here and some additional updates of the Equation indexing has been made. We have rephrased this paragraph to read ' An additional correction term, second term in Eq. (9), accounts for the non-local contributions from local contributions on the EMEP edge grids, those parts of the EMEP grids that are outside the moving window and not included as a local contribution in Eq. 6. In those cases the local EMEP contribution outside the moving window must be converted to a non-local contribution and subtracted from the calculated non-local value, first term in Eq. 9.'. These are geometrical arguments that are difficult to explain with words and equations but we hope the concept has become clearer.

- Eq 10: Why the division by n_{source} ?

* This was also commented by reviewer 1 and we have rewritten the text and reformulated Eq. 10 to make this clearer. The term n_{source} was used to average $CG(i,j,s)$ since this value contains non-local contributions from other sources as well, each source having its own local and non-local contribution. In addition the term $CG(i,j,s)$, in Eq. 10, was actually never defined (it is $CG(i,j,s) = CG_{local}(i,j,s) + CG_{nonlocal}(i,j,s)$). The text now reads, 'These local and non-local calculations are carried out for each emission source individually so the non-local contribution is also dependent on source and the non-local component for any particular source will also contain the local contributions from the other sources. This makes creating a final non-local contribution complicated. To solve this, all the source specific $CG_{local} + CG_{nonlocal}$ contributions are averaged and the sum of the CG_{local} source contributions are subtracted to obtain the final $CG_{nonlocal}$. The final non-local contribution at each sub-grid $CSG_{nonlocal}$, Eq. (1), is equivalent to the EMEP non-local $CG_{nonlocal}$ contribution and is calculated by ...'

- line 291: This is the first occasion that time is explicitly mentioned, worth a sentence of explanation since so far everything was stationary.

* We have made this clearer by writing 'pollutant travel time (t) from source'.

- Section 3.2: Annual mean with rotationally symmetric Gaussian plume – As the authors state, the condition of homogeneous distribution of wind speeds in all directions is typically not met. A calculation with wind roses would not add too much in complexity but would avoid this assumption

1430 * Yes, wind rose calculations could be made but this does require use of the hourly meteorological data at every point in space within the model domain. This is much more complicated and time consuming than this simple analytical methodology. Comparisons with hourly calculations, Section S5.1, show the assumption works quite well.

- Line 510: traffic emissions are often described as line sources in emission inventories.

1435 What is then the appropriate uEMEP subgrid size?

* We find 25 m is sufficient resolution (around the width of a multi-laned road) and little is gained by higher, or even slightly lower resolutions, see Section S5.3. We use 25 m for receptor calculations though 25 m is prohibitive for large scale map making.

1440

- Which source sectors are included in the uEMEP for Norwegian forecasts?

* This is stated in Section 4.2

1445 - Section 5.1: Are all station types included in the validation? How different is the performance of uEMEP, does it work equally well for street canyon stations as for urban background sites? It would be interesting to indicate the station types in Fig 10a.

* All stations are included. In Norway there are very few traffic stations that could be called 'street canyon', around 3 of these. The rest are in fairly open road situations. There are also very few urban background sites, around 3 of these as well. Since this article is primarily a model description we tried to reduce the validation to a minimum. We believe that a more detailed assessment is more appropriate for a separate paper which includes many more years of data and a more thorough investigation. For the moment the authors think the current validation is sufficient.

1455 - Section 5.1.2: While the agreement is clearly better than with EMEP, still the correlation is quite low and there is a low bias. What is the authors' explanation, given that emissions are provided at quite high resolution? In particular for the low bias in summer, which is also seen in PM2.5 (factor 2!) – is this a regional issue (also seen in EMEP validation against background sites) or a problem in downscaling?

1460

* Without having direct proof we believe the low values in the summer are due to too low estimates of secondary organics in EMEP and not a problem with local sources. This is being looked at. The spatial correlation for PM2.5 annual mean is $r^2=0.49$, which is significantly better than EMEP and given the complexities of PM emissions and processes a reasonable result. Low

correlation for PM10 is dependent on all the same PM2.5 uncertainties but in addition, in Norway and other Scandinavian
1465 countries, road dust emissions have a significant impact on PM10. This emission source is very difficult to model, though we
do use the NORTRIP road dust model for this which is currently state of the science. As mentioned in the previous answer we
will be investigating these problems in a later study that concentrates on the results rather than the model.

- line 66 typo: provided

1470

* Done

- line 130 replace then with comma

1475 * Done

- line 135 the same

* Done

1480

- line 141 add comma after (I,J) to increase readability

* Have added a comma on both sides, I think that is correct.

1485 - line 154 correct reference

* Done

- line 167, 176 the same

1490

* Cannot find this line reference

- line 250 insert comma after 'this' to increase readability

1495 * Done

- Line 305: Define u*.

* Done 'friction velocity'

1500

- Line 406 references missing

* Done

1505 - line 574 reference missing

* Done

1510

1515

1520

1525